NOAA Technical Memorandum NMFS-NE-115

Status of Fishery Resources off the Northeastern United States for 1998

U. S. DEPARTMENT OF COMMERCE
National Oceanic and Atmospheric Administration
National Marine Fisheries Service
Northeast Region
Northeast Fisheries Science Center
Woods Hole, Massachusetts

September 1998

Application of a 2-D Particle Tracking Model to Simulate Entrainment of Winter Flounder Larvae at the Millstone Nuclear Power Station

by
Nadia K. Dimou
and
E. Eric Adams

Energy Laboratory Report No. MIT-EL 89-002
November 1989

Application of a 2-D Particle Tracking Model to Simulate Entrainment of Winter Flounder Larvae at the Millstone Nuclear Power Station

by

Nadia K. Dimou

and

E. Eric Adams

Energy Laboratory

and

R. M. Parsons Laboratory
for Water Resources and Environmental Engineering
Department of Civil Engineering

Massachusetts Institute of Technology

Cambridge, MA 02139

sponsored by

Northeast Utilities Service Co.

under

MIT Energy Laboratory Electric Utility Program

Energy Laboratory Repart No. MIT-EL 89-002

October 1989 (draft)

November 1989 (final)

Abstract

A 2-D random walk model, developed by Dimou (1989) as part of this research project, was used to simulate entrainment at the Millstone Nuclear Power Station of winter flounder larvae hatched within Niantic River.

Important features of the model include larval behavior (vertical migration as a function of time of day and tidal stage) and tidal dispersion within Niantic River which was calibrated to Ketchum's (1951) Modified Tidal Prism Model. Simulations using larval hatching rates inferred from the densities of yolk-sac larvae collected within the river showed the larvae arriving significantly earlier and in smaller numbers than indicated by observations at the intake. A dye study conducted within the river and available salinity data showed that the hydrodynamic flushing time is actually less than it was simulated to be, so this does not explain the discrepancy in arrival times. However, dates of peak abundance for larvae collected at different locations within the river and Niantic Bay imply that actual larval retention times may be significantly greater than the hydrodynamic residence time, suggesting that adjustments may need to be made in the representation of larval behavior. A second dye study, conducted in the bay, showed that 15-25% of water exiting the river mouth passes through the intake—in excellent agreement with simulations.

Additional factors that could help explain the small entrainment numbers and early arrival times simulated by the model are briefly discussed and include the possibilities that larval hatching rates are too low, possibly due to the method of sampling yolk-sac larvae; simulated mortality rates are too high; and larvae are being imported to the region from different spawning areas.

Acknowledgment

This report consists essentially of the application portion of the Masters Thesis of Nadia Dimou, entitled "Simulation of Estuary Mixing Using a Two-Dimensional Random Walk Model." The thesis was supervised by Eric Adams of MIT's Dept. of Civil Engineering and was submitted in July 1989. The research was supported by Northeast Utilities Service Company. The authors would like to thank NUSCo for their financial support and to express their gratitude to Ernesto Lorda, Dale Miller, Don Donella, and Linda Bireley of the Northeast Utilities Environmental Lab at Millstone, who were always helpful throughout the study.

1 Purpose and Scope

The purpose of this report is to describe application of the model MILL, a two-dimensional random walk model used to simulate the entrainment of winter flounder larvae at the Millstone Nuclear Power Station (MNPS) (Figure 1). Several shallow areas in the vicinity of MNPS (including Niantic River and Outer Jordan Cove) serve as spawning areas for winter flounder. A fraction of larvae, hatched in these areas, is expected to be entrained, and hence killed, through entrainment at the station.

2 Background

The large effort devoted to winter flounder studies is related to its importance for the Connecticut sport and commercial fisheries. It is the most valuable commercial finfish in Connecticut and on average makes up about 20% of the total finfish landings. The winter flounder is also one of the most popular marine sport fishes in the state with an estimated annual catch in 1979 of almost 1.4 million fish with a total weight of 412,243 kg. Its particular life history also makes it potentially susceptible to various types of impacts (NUEL Annual Report 1988).

The MNPS is located on the north shore of Long Island Sound in Waterford, Connecticut (Figure 1). The station consists of three operating units: Millstone Unit 1 commenced commercial operation in 1970, Unit 2 in 1975, and Unit 3 in 1986. Extensive studies of the potential impacts of MNPS on local marine flora and fauna have been conducted since 1968. During this period studies have consistently been reviewed and updated to assure that the best available methods were used. Preliminary field studies to estimate abundance of the winter flounder population in 1973-74 were expanded in scope in 1975, when surveys using mark and recapture techniques were initiated. An adult abundance survey has been completed each year through the

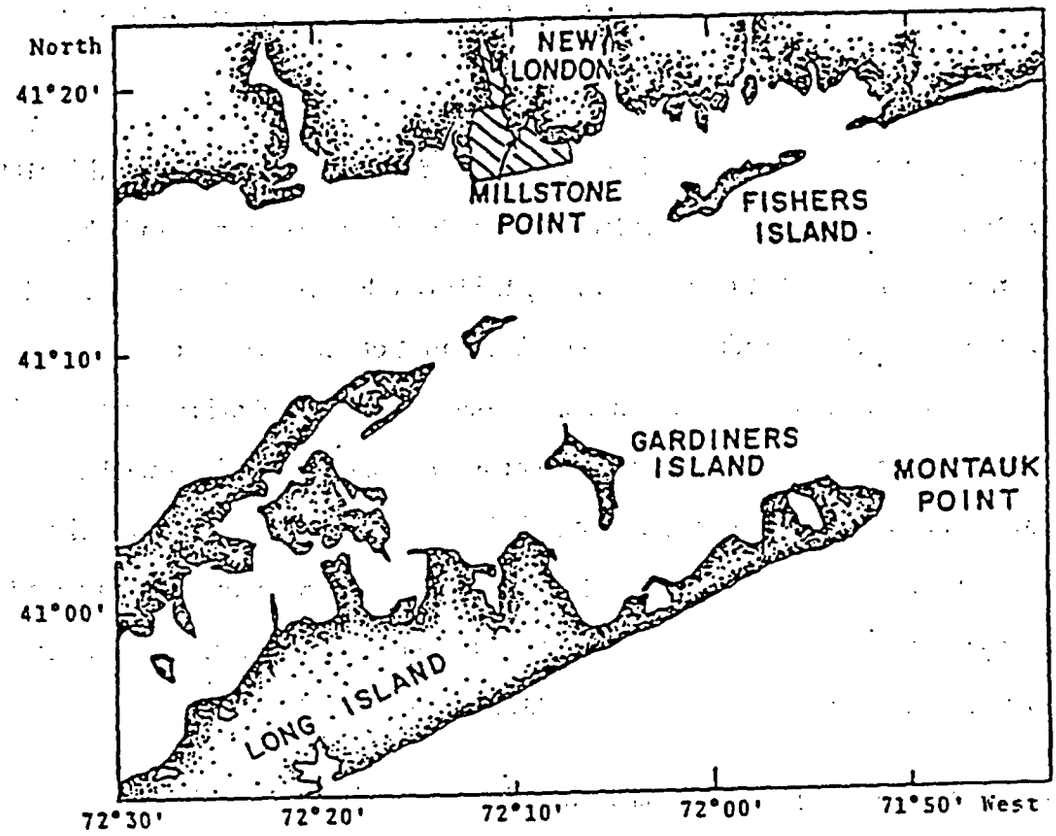

Figure 1 Location of Millstone Nuclear Power Station (from Saila, 1976, Figure 1)

present. In many years, studies of age structure, reproductive activity, growth, survival, movements, early life history, and stock identification were conducted. For plant impact, impingement and entrainment estimates are available for each year (NUEL Annual Report 1988). Data from many of these studies have been used in a predictive mathematical population dynamics model developed by the University of Rhode Island (Saila, 1976). This model formed the basis for earlier MNPS impact assessments, including that for Unit 3.

The present analysis is based on the MIT model MILL (Dimou, 1989). Model MILL is a two-dimensional random walk model based on the Eulerian-Lagrangian finite element transport model ELA (Baptista et al., 1984) coupled with the harmonic finite element model TEA (Westerink et al., 1984). The input of the model consists of the continuous distribution of larvae hatching over time, the larval behavior as a function of age, tidal and diurnal phase, and natural mortality. The output of the model gives the locations and fate of the larvae at specified time intervals after the start of the simulation. As described in more detail, MILL is similar in many ways to Saila's model (1976) but also includes some major differences. The major differences between the model MILL and the model used by Saila (1976) are the following:

1) Differences in grid used: MILL is a finite element model and uses irregular, triangular grid elements whereas Saila's model is a finite difference model and uses regular, square grid elements. This configuration allows for easy grid refinement in critical regions, such as the Niantic River and the plant intake area (Figure 2).

2) Differences in larval distribution: In Saila's analysis larvae were hatched instantaneously over a prescribed spatial distribution whereas in MILL larvae are hatched over a 2-month period in three stations A, B, C (Figure 3) according to temporal and spatial distributions provided by NUEL.

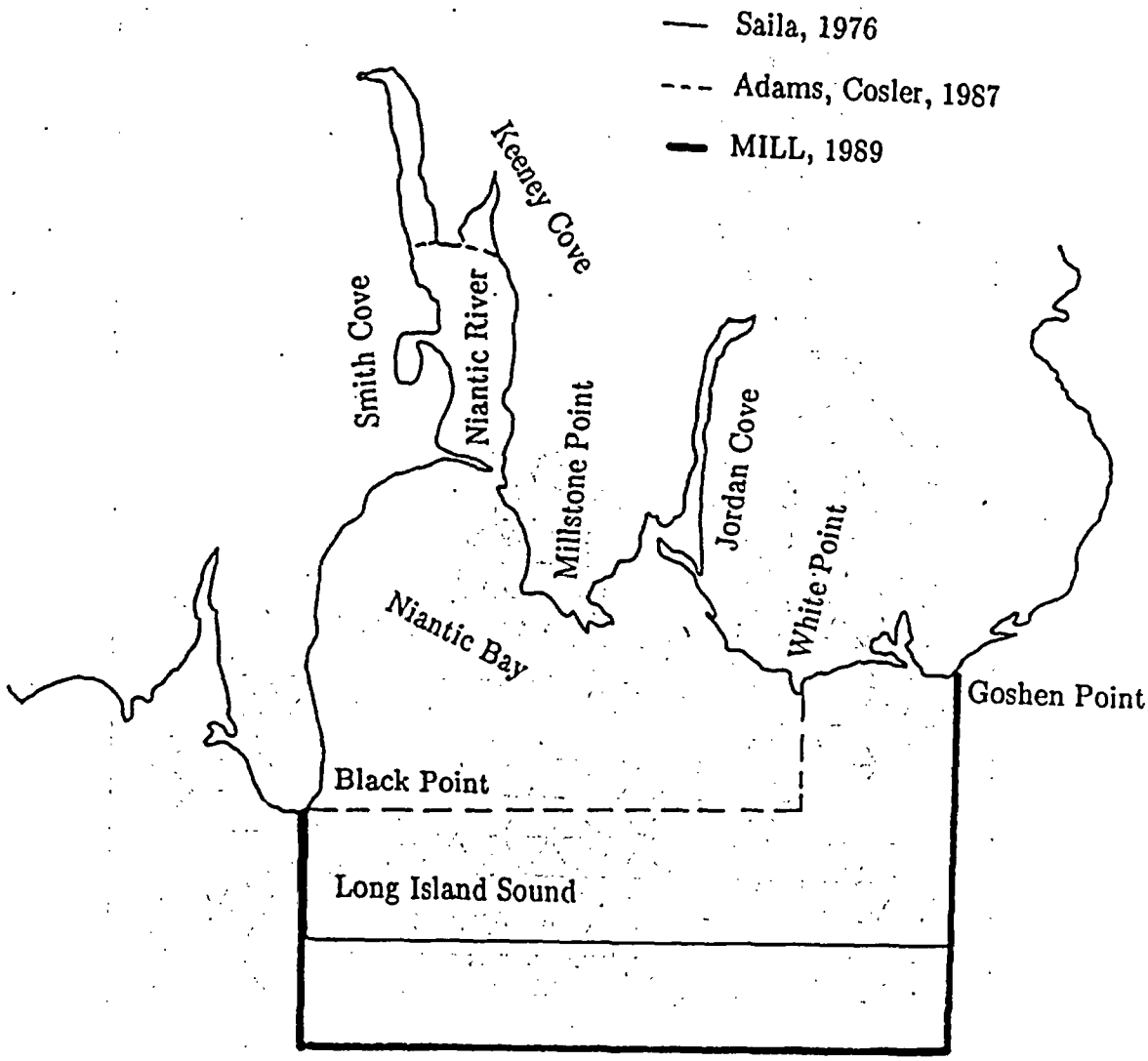

Figure 2 Comparison between the three grids

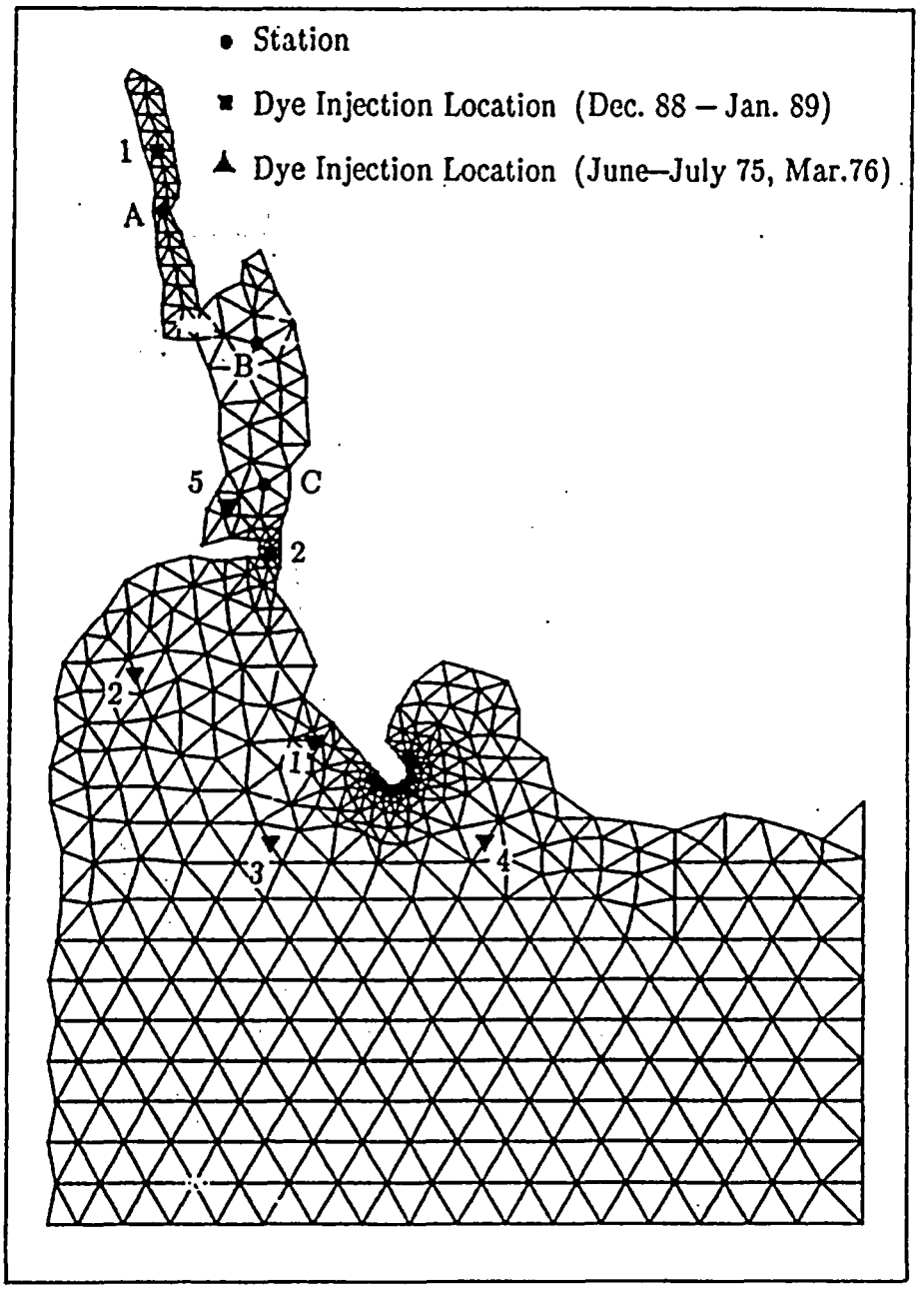

Figure 3 Locations of Stations A, B, C. Dye injection locations for dye studies conducted in December 1988 - January 1989 and June-July 1975, March 1976

3) Differences in larval behavior: In Saila's analysis larvae were passive (i.e., they follow the motion of the water) throughout their development. However according to studies larvae show a specific tidal and diurnal behavior that is a function of their age. This behavior is simulated in model MILL.

4) Difference in model: Saila uses an Eulerian model, where larvae are simulated as mass of larvae and concentration is found at every grid point. This model uses a Lagrangian approach, where larvae are simulated by particles and followed around the waterway. The location of these particles is found at every timestep. Saila (1976) notes the potential advantages of the Lagrangian approach, but he does not follow this approach because of the long computer times required. MILL takes advantage of newly developed computational methods, which provide higher speed for extended simulations.

3 Grid

The Millstone grid used to study the thermal plume at Millstone (Adams and Cosler, 1987) was extended to include the northern reaches of Niantic River where larvae are hatched (Station A) (Figure 3). It was also extended further south and east in Niantic Bay to enlarge the domain, thus reducing the frequency of simulated larval losses at the open boundaries. Figure 2 shows the domains covered by the different grids used in the Millstone area: 1) the grid used by Saila (1976), 2) the grid used by Adams and Cosler (1987), and 3) the grid used in this study. Figures 3 and 4 show the grid used in this study and the locations of:

- Larvae hatching stations A, B, C (see Section 6)
- Current water stations, tidal meter stations, tide gauge stations (see Section 4)
- Dye injection locations for studies in 1975-1976 (see Section 9)

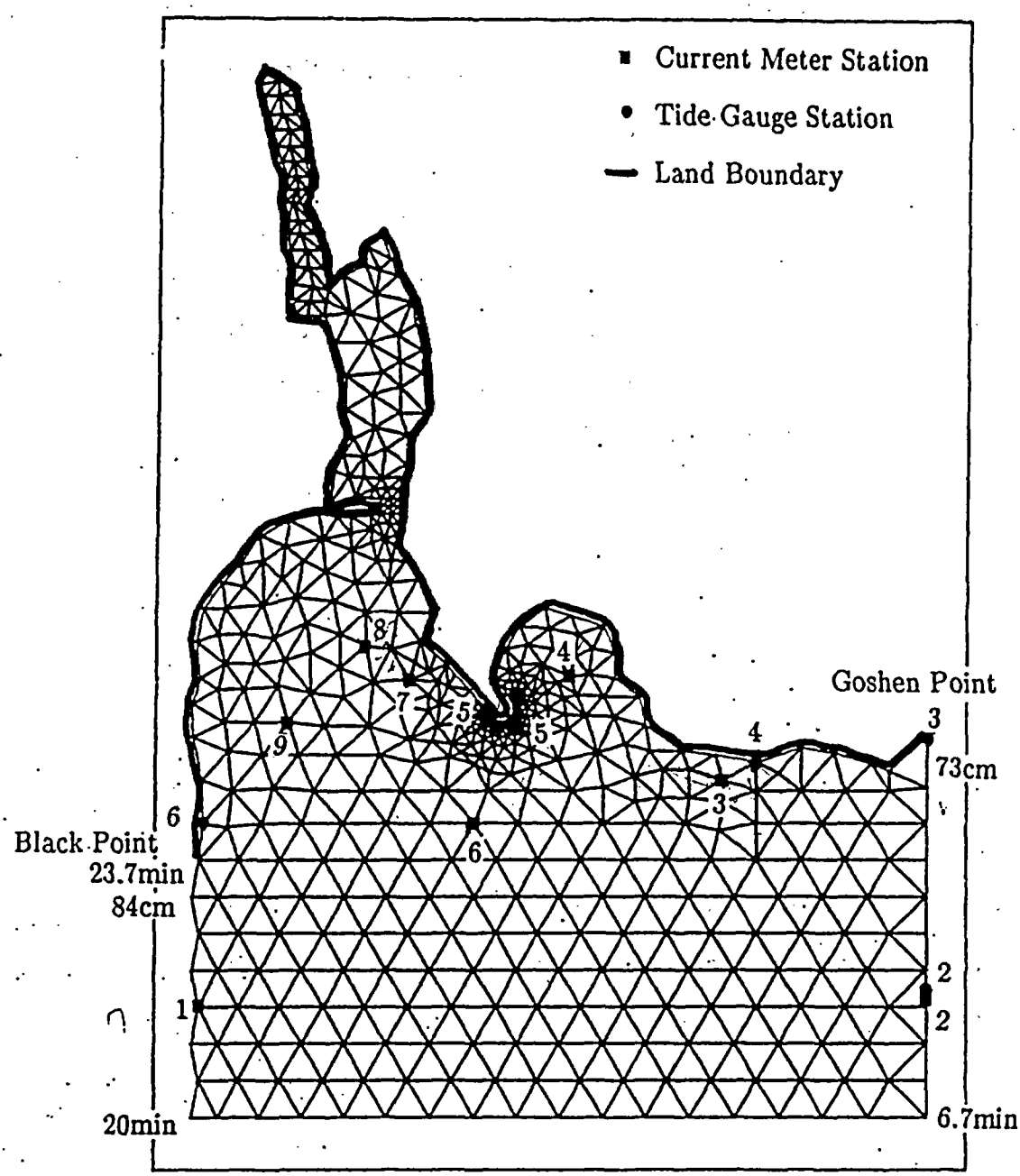

Figure 4 Current meter locations, tidal current meter locations, tide gauge locations

- Dye injection locations for studies in 1988-1989 (see Section 9)

4 Flow Model

4.1 General

The linear version of the two-dimensional (depth-averaged) harmonic finite element circulation model TEA was used. The equations to be solved are the depth-averaged continuity and Navier-Stokes equations under the assumption of constant fluid density, small tidal amplitude, hydrostatic pressure distribution, negligible convective acceleration and momentum dispersion, and constant pressure at the air-water interface (Westerink et al., 1984). These equations are

$$\eta_t + (uh)_x + (vh)_y = 0 \tag{1}$$

$$u_t + gn_x - fv - \frac{1}{\rho h}(\tau_x^s - \tau_x^{b,lin}) = 0 \tag{2}$$

$$v_t + gn_y - fu - \frac{1}{\rho h}(\tau_y^s - \tau_y^{b,lin}) = 0 \tag{3}$$

where

u,v are the depth-averaged velocities in the x and y directions respectively

η is the surface elevation above the mean water level

h is the mean water depth

t is the time

g is the acceleration due to gravity

ρ is the density of water

f is the Coriolis parameter

τ_x^s and τ_y^s are the surface stresses in the x and y directions respectively

$\tau_x^{b,lin}$ and $\tau_y^{b,lin}$ are the linearized bottom stresses in the x and y directions respectively

The bottom friction has been linearized as

$$\frac{T_x^{b,lin}}{\rho} = \lambda u \quad \text{and} \quad \frac{T_y^{b,lin}}{\rho} = \lambda v \tag{4}$$

λ is the linearized friction coefficient and has the form

$$\lambda = u_{max} \frac{8}{3\pi} c_f \tag{5}$$

where

u_{max} is the representative maximum velocity during a tidal cycle

c_f is the friction factor.

The following assumptions were made:

- No tributary inflows. Average freshwater inflow from Lattimer Brook and Jordan Brook are about 10 cfs and 2 cfs respectively and generally have a negligible effect on circulation compared to tidal currents.

- Circulation induced by winds was ignored because they generally have only a secondary influence on the circulation (Saila, 1976). Furthermore, the effects of extreme winds are manifest in vertical as well as horizontal gradients of velocity; the former are not properly represented in a depth-averaged model. To the extent they are important, both freshwater inflow and wind-driven circulation must be accounted for by mixing in the transport model.

For the simulation of the flow in Niantic River and Bay two runs of TEA were necessary. In the first run the tidally induced circulation was simulated. In the second run the steady-state depth-averaged circulation due to the operation of the three units was simulated following Adams and Cosler (1987). The result of the two runs were superimposed.

4.2 Boundary Conditions

For specifying the boundary conditions, data from two hydrographic surveys, conducted during summer (8 Aug to 10 Sept, 1973) and winter (6 to 20 Feb, 1974), were used. The data from the tide elevations were used to specify tide amplitude and phase lag at the boundary nodes and velocity current data were used to check the accuracy of the model. In Figure 4 the configurations of shoreline tide gauging stations and current meters for the winter survey are shown.

As shown in Figure 4 there are not enough tide elevation data in order to specify boundary conditions for the present domain. So the boundary conditions were chosen to achieve a reasonable fit in terms of flood and ebb current speed and direction.

The tide range was taken to increase linearly across the boundary from the value $R_1 = 73$ cm at Goshen Point to the value $R_2 = 84$ cm at Black Point (Figure 4); i.e., $\eta = R_1 + x(R_2-R_1)$ where x is the dimensionless distance from Black Point to Goshen Point.

The phase lag ϕ was also chosen to vary linearly from Goshen Point to Black Point with the tide arriving at Goshen Point 23.2 min later than at Black Point (Figure 4).

A constant friction factor of $f = 0.0001$ was used.

In Figure 5 the flow field due to tidal currents at time t = 3.1 h after high tide is plotted.

4.3 Intake and Discharge Flux Conditions

The condenser water intake flow for three units is about 118 m^3/sec. This flux was evenly distributed among four nodes (Figure 6). Adams and Cosler (1987) calculated that the near field volumetric dilution due to the surface discharge is about 3. Therefore the plume entrainment rate is twice the intake flow rate and is evenly distributed among three entrainment nodes on the left and three entrainment nodes on the right of the discharge. The discharge is distributed among four nodes (Figure 6). In Figure 7 the flow field due to the steady-state operation of the three units is plotted.

In Figure 8 the flow field from the superposition of the flow fields of Figures 5 and 7 is plotted.

5 Transport Model

A two-dimensional depth-averaged particle tracking (random walk) transport model was used (Dimou, 1989). In this approach, the change in the position (x,y) of a particle (or larva), during time interval Δt, is given by a combination of deterministic and random movements according to the following step equations

$$\Delta x = \left[\frac{D_{xx}}{h}\frac{\partial h}{\partial x} + \frac{\partial}{\partial x} D_{xx} + u\right]\Delta t + \sqrt{2D_{xx}\Delta t}\, z_n \qquad (6)$$

$$\Delta y = \left[\frac{D_{yy}}{h}\frac{\partial h}{\partial y} + \frac{\partial}{\partial y} D_{yy} + v\right]\Delta t + \sqrt{2D_{yy}\Delta t}\, z_n \qquad (7)$$

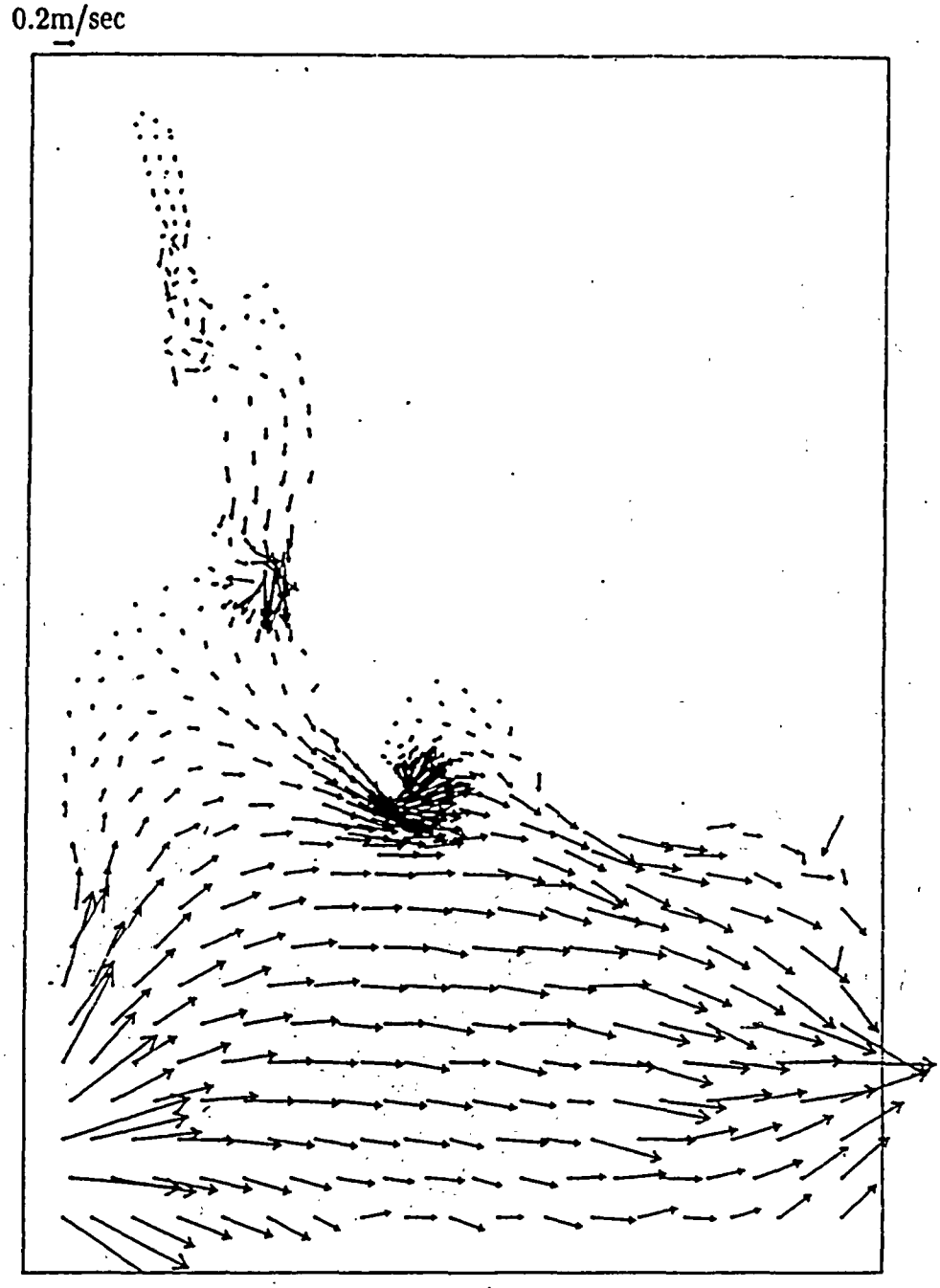

Figure 5 Flow field due to tidal currents at time t = 3.1 h after high tide

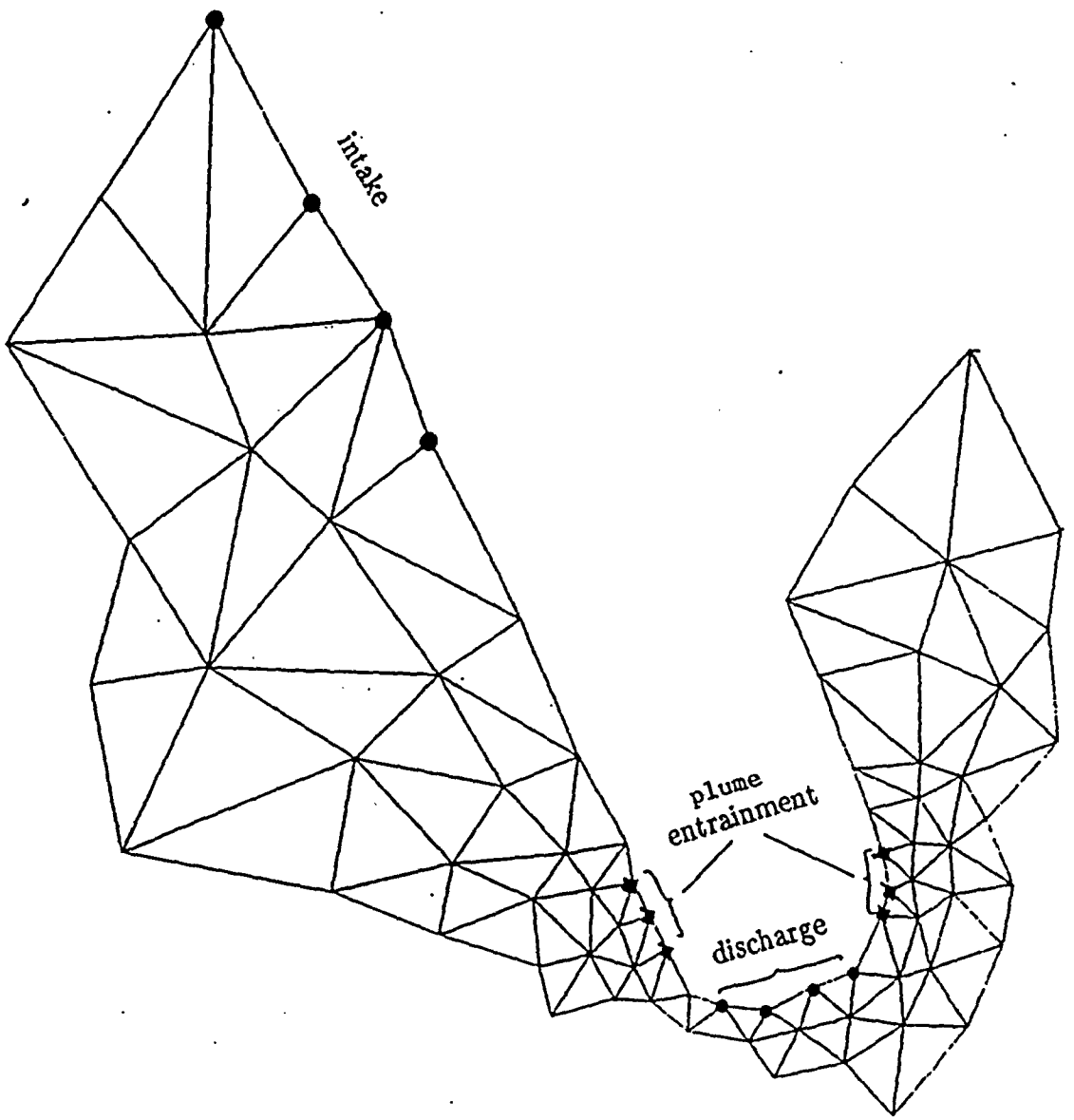

Figure 6 Intake and discharge

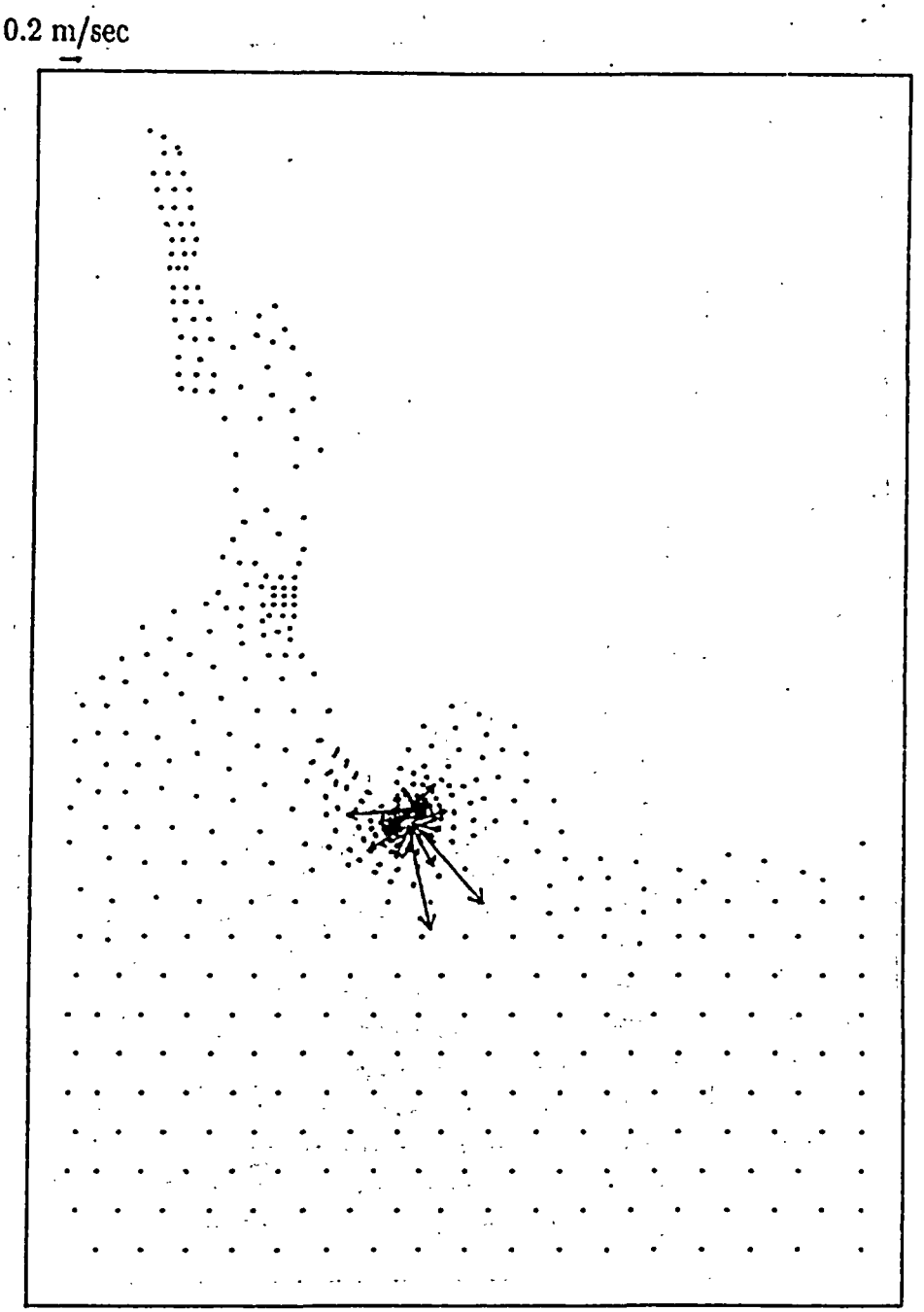

Figure 7 Flow field due to steady-state operation of the three units

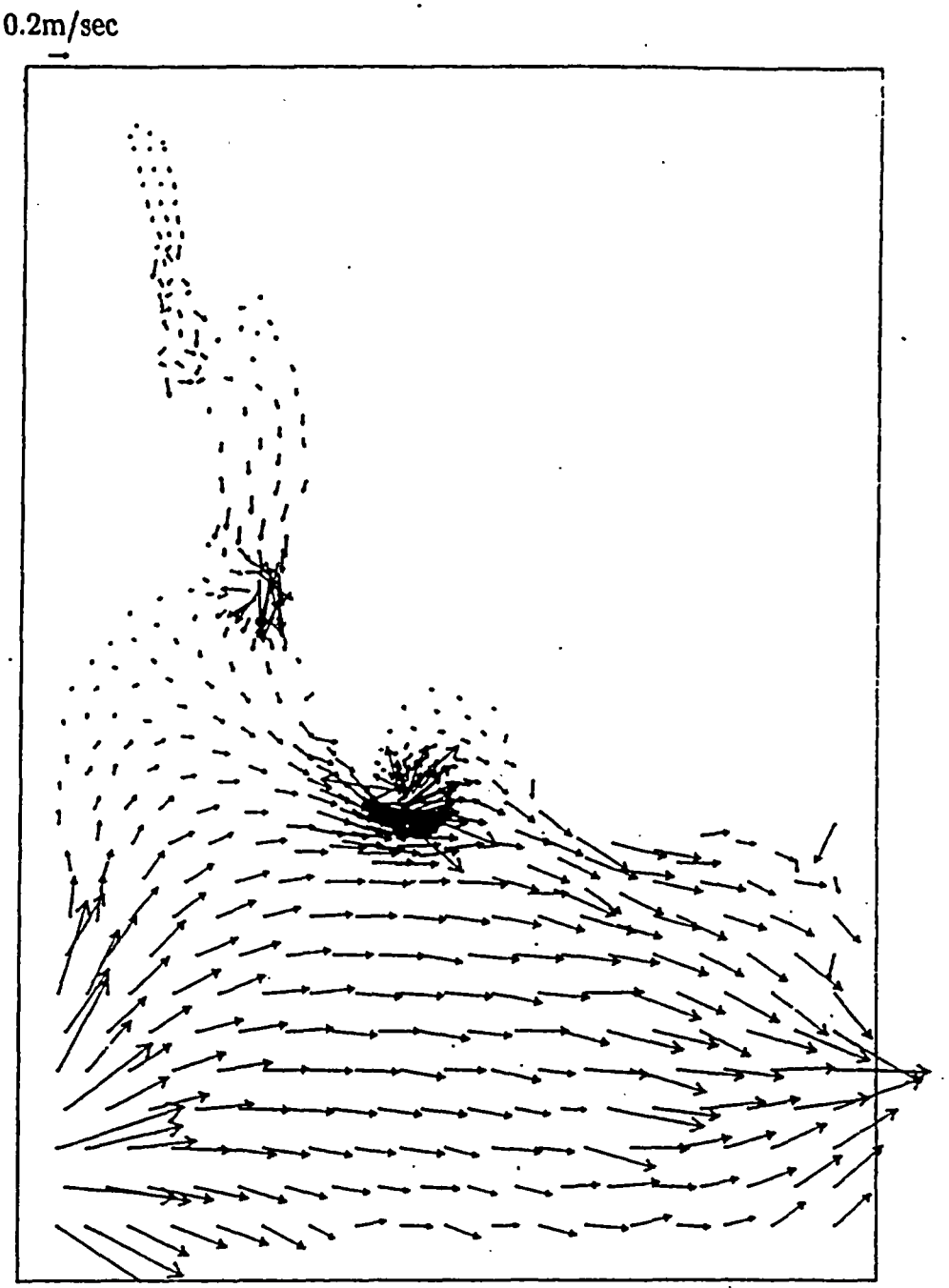

Figure 8 Flow field from superposition of flow fields of Figures 20 and 22

where D_{xx} and D_{yy} are dispersion coefficients along (principal) axes x and y, h is water depth, u and v are depth-averaged velocities (e.g., from TEA) and z_n is a random number with zero mean and unit variance. It remains to specify D_{xx} and D_{yy}. In order to do that the domain was divided into two regions: Niantic River and Niantic Bay.

Niantic River was treated as an estuary using mixing length theory (Arons and Stommel, 1951; Officer, 1976). According to this tidal mixing is represented by a longitudinal dispersion coefficient given by

$$D = \beta u_0^2 \tag{8}$$

where u_0 is the amplitude of the tidal velocity. Since the dispersivity tensor is diagonal we can evaluate D_{xx} and D_{yy} using the expressions

$$D_{xx} = \beta u_0^2 \tag{9}$$

$$D_{yy} = \beta v_0^2 \tag{10}$$

where

u_0 and v_0 are the maximum tidal velocities in the x and y direction respectively

Thus the random walk algorithm is given by

$$\Delta x = \left[u + \beta \frac{u_0^2 \partial h}{h \partial x} + \frac{\partial(\beta u_0^2)}{\partial x}\right]\Delta t + \sqrt{2\beta}\, u_0 \sqrt{\Delta t}\, z_n \tag{11}$$

$$\Delta y = \left[v + \beta \frac{v_0^2 \partial h}{h \partial y} + \frac{\partial(\beta v_0^2)}{\partial x}\right]\Delta t + \sqrt{2\beta}\, v_0 \sqrt{\Delta t}\, z_n \tag{12}$$

where u and v in Equations (11) and (12) are the steady state velocities from the plant operation.

The gradients $\frac{\partial h}{\partial x}$, $\frac{\partial h}{\partial y}$, $\frac{\partial(\beta u_0^2)}{\partial x}$, $\frac{\partial(\beta v_0^2)}{\partial y}$ are estimated at every node using a finite element code. For estimating these gradients at intermediate points in the domain, quadratic interpolation functions are used. The deterministic component of the random walk algorithm is estimated using the fifth-order Runge-Kutta method used in ELA (Baptista et al., 1984).

The mixing parameter β in our model for Niantic River was computed to be consistent with Ketchum's (1951) theoretical model of tidal mixing. The reason for referencing Ketchum's model is that it can be used for estimating longitudinal concentration distributions and flushing times in estuaries of irregular geometry and bathymetry. Ketchum's model has been previously used for the prediction of flushing times and longitudinal salinity distributions in Niantic River (Kollmeyer, 1972), but without any field verification. It should be pointed out that Ketchum's model, known as the modified tidal prism method, does not explicitly use a dispersion coefficient. Instead the method divides the estuary into a number of longitudinal segments, of length equal to the local tidal excursion. By assuming complete mixing in each segment over a tidal cycle, one can compute an effective dispersion coefficient. Following Arons and Stommel (1951), who examined estuaries of uniform crossection, the theoretical value of β consistent with Ketchum's model is $\beta = T/\pi^2$.

Because β was computed from Ketchum's theoretical model, it was useful to compare modeled residence times with those computed with Ketchum's analytical model. Accordingly, Ketchum's model was used to compute residence times corresponding to the location of dye injection from Study 1 conducted in Niantic River in 1988 (Figure 3). (Bathymetric data were obtained from Kollemyer, 1972; see Section 9 for a detailed description of the dye study.) The computed residence time was 15 days and the model segmentation is shown in Figure 9.

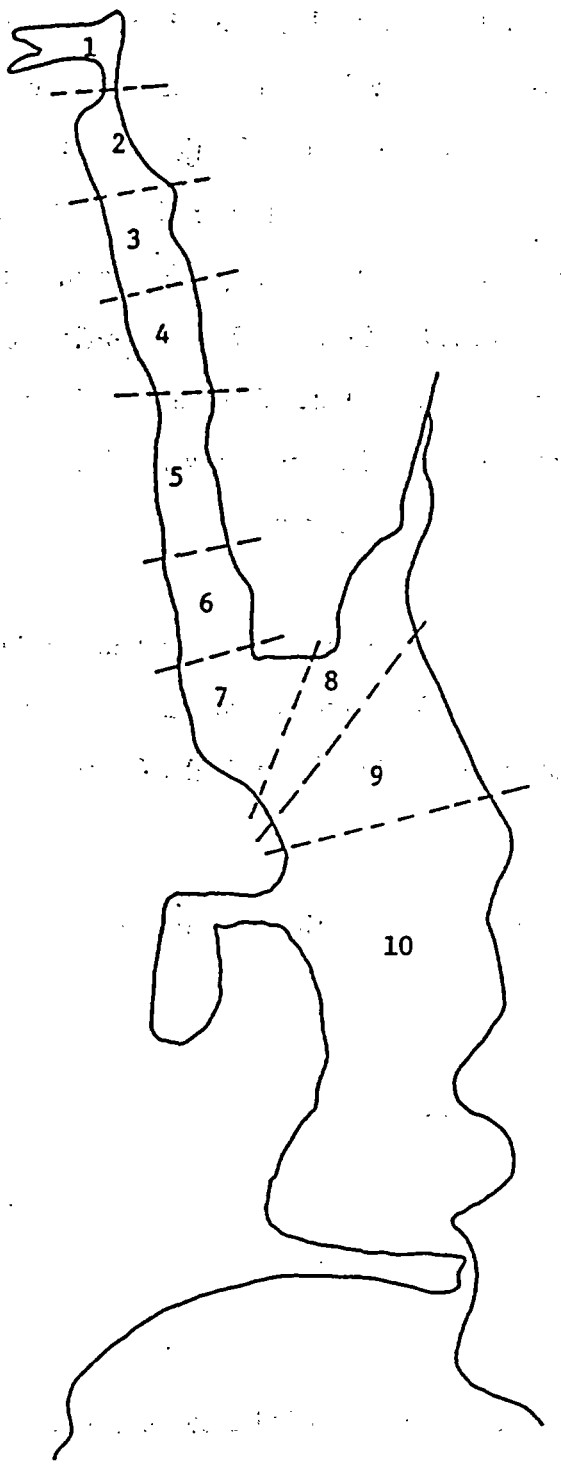

Figure 9 Estuary segmentation using Ketchum's model

This theoretical estimate can be compared with our model flushing time in the following way. Several particles are released at the injection point. For each of these particles a residence time is recorded. By residence time we mean the time it takes for a particle to leave the estuary (pass south of Mijoy Dock). As flushing time of the estuary we designate the mean of the resulting residence time distribution. The flushing time from the model MILL (using dispersion coefficents, i.e., value of β, based on Ketchum's model) is equal to 14 days. The small difference with Ketchum's analytical method may be due to the fact that we are using an ideal geometry for calibrating the parameter β, while for estimating the flushing time we are using the actual irregular geometry and bathymetry.

Niantic Bay was assumed to have a constant dispersion coefficient $D_{xx} = D_{yy} = D$. The value of 21.9 ft^2/sec from Saila's model was used. The advective velocities u and v were obtained from the superposition of the tidal velocities and the velocities from the power plant operation.

Accordingly, the random walk algorithm is given by

$$\Delta x = u\Delta t + \sqrt{2D}\sqrt{\Delta t}\, z_n \tag{13}$$

$$\Delta y = v\Delta t + \sqrt{2D}\sqrt{\Delta t}\, z_n \tag{14}$$

6 Modeling Larval Behavior

6.1 General

Larval growth and behavior are modeled according to data provided by NUEL. This information is based on field data collected from Niantic River and Bay and includes

- estimates of the temporal and spatial distribution of yolk-sac larvae from which hatching rates may be estimated
- daily growth rates as a function of temperature
- average weekly water temperature
- daily larval survival rates as a function of age
- diel and tidal behavioral responses as a function of larval size
- mortality due to entrainment as a function of larval size

The general approach followed in the simulations is the following. Particles are released at a fixed rate from several points in space that approximate a spatial distribution of hatching of winter flounder larvae. Each particle represents a certain number of larvae corresponding to the temporal distribution of hatching winter flounder larvae. The larvae in each "larval cohort" represented by one particle may have one of the following fates:

- Die because of natural mortality.
- Go through the intake. In this case, if the length of the larvae in the cohort is less than 7 mm we have 100% mortality so we stop tracking the particle. Otherwise we have 20% mortality so the particle is placed in the discharge plume and we continue tracking the particle that now represents 20% fewer larvae than in the timestep before entrainment.
- Go out of the model boundary (i.e., are flushed out) in which case tracking stops.

- Reach the length of 8 mm. In this case larvae are considered juveniles and we stop tracking them.

According to the above, if we designate the survival factor SF(i,t) as the fraction of larvae in cohort i which are alive and in the domain at time t after they were hatched, then SF(i,t) is given by the expression

$$SF(i,t) = NSF \cdot ISF \cdot FSF \cdot JSF \tag{15}$$

where

NSF is the natural survival factor or the fraction not dead due to natural mortality

ISF is the intake survival rate. It can take the following values:

ISF = 1 if the particle representing the larvae cohort did not go through the intake

ISF = 0 if the particle representing the larvae cohort goes through the intake and the length of the larvae is less than 7 mm

ISF = $(0.8)^n$ if the particle representing the larvae went through the intake n times and the length of the larvae was more than 7 mm the first time it was entrained

FSF is "flushing" survival rate that takes the values 0 or 1 if the particle has or has not been flushed out of the domain

JSF is the "juvenile" survival factor that takes the value 0 if the larvae reach the length of 8 mm; otherwise it is equal to 1

6.2 Larval Hatching Distribution

Estimated larval hatching was based on the abundance of yolk-sac larvae (larvae less than ten days old) in the Niantic River at Stations A, B, C (Figure 3) during 1984-

87. Abundance is expressed as density/500m^3. Figure 10 shows the average temporal abundance of yolk-sac larvae for the four-year period for Stations A, B, and C.

Daily larval hatching rates were estimated from daily abundance data according to the following procedure. If we call N(i,10) the cumulative number of larvae hatched per 500 m^3 during the 10 days preceding day i and still alive at the start of day i, then

$$N(i,10) = B(i) \sum_{t=1}^{10} S(i)^t \tag{16}$$

where B(i) and S(i) are the *constant* daily rates of hatching and survivability, respectively, during the time from t = 1 through t = 10 (day i-10 through i-1), and k is the natural mortality rate for larvae less than 10 days old. Using k = 0.105 d^{-1} (NUEL, personal communication),

$$S(i) = e^{-.105} = .90 \tag{17}$$

and solving for B(i), we have

$$B(i) = \frac{N(i,10)}{.90 + .90^2 + \cdots + .90^{10}} \tag{18}$$

or

$$B(i) = 0.17N(i,10) \tag{19}$$

i.e., the daily hatching rate is about 17% of the yolk-sac abundance ten days later.

In the simulations a 3-hr timestep is used, so according to Equation (19) the number of larvae b(t) born in every 3-hr timestep is given by

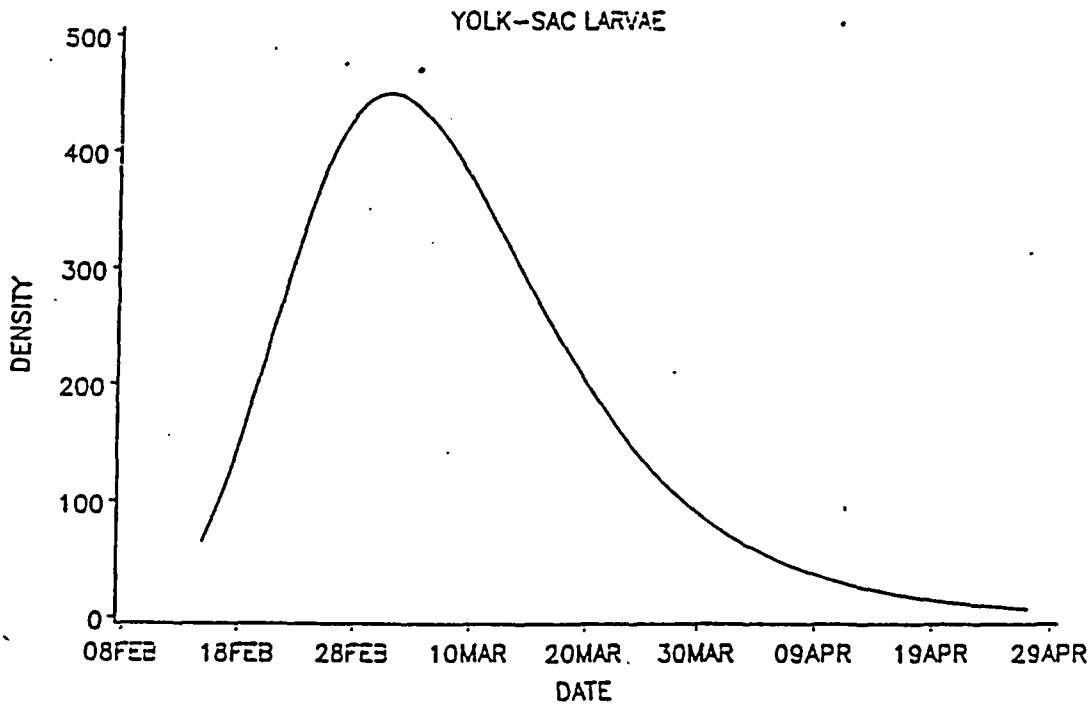

Figure 10 Average temporal abundance of yolk-sac larvae for the period 1984-87 for stations A, B, and C (data from NUEL)

$$b(t) = \frac{B(i)}{24/3} = 0.0213N(i, 10) \quad (20)$$

Figure 11 shows the average birthrates (number of larvae born per day in 500 m^3) for the period 1984-87 for Stations A, B, and C. Integrating over time and the respective volumes associated with the three stations, the total number of larvae simulated to be hatched is about 22×10^6.

6.3 Larval Growth Rate

Annual larval growth rates were calculated by NUEL from twelve years (1976-87) of entrainment data and the annual rates were found to be correlated to seasonal water temperatures. According to these data the growth rate in units of mm/day is given as a function of temperature by the following expression

$$\text{mm/day} = \frac{dL}{dt} = -0.0145 + 0.0134T \quad (21)$$

where T is given in °C.

It was assumed that the length of the larva at the time it is born is 3 mm.

6.4 Daily Survival Rates

According to data the average daily survival factor was taken equal to 0.90 for larvae of length between 3-4 mm and 0.97 for longer lengths.

6.5 Diel Behavioral Response

According to a comparison of samples collected during daylight and at night, larvae become less available to capture during daylight as they increase in length. Larvae

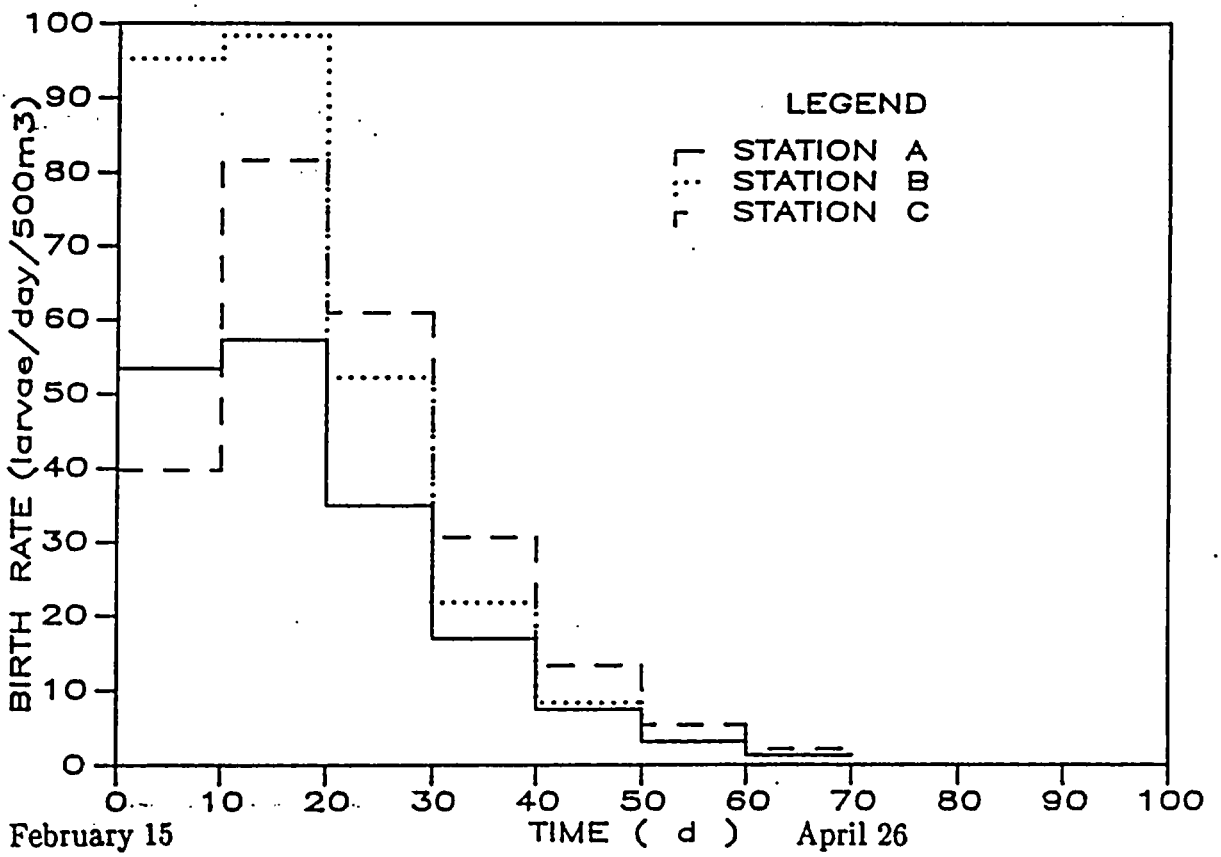

Figure 11 Averaged birthrates (number larvae born per 3 hr in 500 m^3) for the period 1984-87 for Stations A, B, and C

begin to develop this diel behavior at about 5 mm in length. The proportion of larvae (y) available for tidal transport during daylight as a function of length is given by the expressions

$$\begin{aligned} y &= 1.0 \qquad (L < 5mm) \\ y &= 0.985 - 0.094 \cdot L \quad (L > 5mm) \end{aligned} \tag{22}$$

This diel behavior was apparent at all stations in the Millstone area except at Station C (Figure 3). Larval diel behavior was simulated as follows. The displacement for larvae of length more than 5 mm that are located in any area in our domain except near Station C was multiplied by the factor y. So Equations (11) and (12) become

$$dx = y\left[u + \beta u_0^2 \frac{1}{h}\frac{\partial h}{\partial x} + \frac{\partial(\beta u_0^2)}{\partial x}\right]\Delta t + y\sqrt{2\beta}\, u_0\sqrt{\Delta t}\, z_n \tag{23}$$

$$dy = y\left[v + \beta v_0^2 \frac{1}{h}\frac{\partial h}{\partial y} + \frac{\partial(\beta v_0^2)}{\partial y}\right]\Delta t + y\sqrt{2\beta}\, v_0\sqrt{\Delta t}\, z_n \tag{24}$$

6.6 Tidal Behavioral Response

Larvae in Station C also show vertical migration, but as a function of tidal stage rather than light: they fall to the bottom during ebb and rise within the water column during flood tide. Again larvae begin to develop this behavior at about 5 mm in length. The proportion of larvae y available for transport during an ebb tide is given by the expression

$$\begin{aligned} y &= 1.0 \qquad (L < 5mm) \\ y &= 1.696 - 0.221 \cdot L \quad (L > 5mm) \end{aligned} \tag{25}$$

Larvae tidal behavior was simulated in the same manner as by diel behavior, i.e., by multiplying the advection and random-walk components by the factor y during ebb for larvae of length more than 5 mm that are located in Station C (Figure 3).

6.7 Alternative Solution for Millstone Case Study

Before proceding, it is worth comparing our random walk model with a concentration or "diffusivity" model which could have been used. The question is what "concentration" represents. It can represent mass of larvae per unit volume of water or number of larvae per unit volume of water. In this case number of larvae per unit volume should be used since we are not interested in the mass of larvae in the domain. The governing transport equation for larval concentration c is of the form

$$\frac{\partial c}{\partial t} + u\frac{\partial c}{\partial x} + v\frac{\partial c}{\partial y} = \frac{1}{h}\frac{\partial}{\partial x}\left[hD_{xx}\frac{\partial c}{\partial x}\right] + \frac{1}{h}\frac{\partial}{\partial y}\left[hD_{yy}\frac{\partial c}{\partial y}\right] + Q \qquad (26)$$

The problem using this method, as written, is that larval behavior can not be modeled. Since larvae show strong behavioral patterns this approach is not appropriate.

Larval behavior *can* be taken into account using a concentration model if a group of equations of the form of Eq. (26) is used

$$\frac{\partial c_i}{\partial t} + u\frac{\partial c_i}{\partial x} + v\frac{\partial c_i}{\partial y} = \frac{1}{h}\frac{\partial}{\partial x}\left[hD_{xx}\frac{\partial c_i}{\partial x}\right] + \frac{1}{h}\frac{\partial}{\partial y}\left[hD_{yy}\frac{\partial c_i}{\partial y}\right] + Q_i \quad i = 1, \ldots n \qquad (27)$$

where c_i is the number of larvae of length group i per unit volume of water $L_{li} < L_i < L_{ui}$, L_{li} and L_{ui} being the lower and upper limit of length of group i. As mentioned before we are interested in larvae of length L = 3 mm (length of larvae at the hatching time) to length L = 8 mm. It is enough if we take five groups, i.e., n = 5 (1-mm increments).

The term Q_i is equal to

$$Q_i = k_{i-1}c_{i-1} - k_ic_i + a \cdot \sum_{i=1}^{1} Q_1 \cdot c_i \, \delta(x-x_1)(y-y_1) + d_ic_i \qquad (28)$$

where

$k_{i-1}c_{i-1}$ is a source term that represents the number of larvae per unit volume per time that reach length L_{1i}

k_ic_i is a sink term and represents the number of larvae per unit volume per time, that reach length L_{ui}

$a \sum_{i=n}^{1} Q_1c_i\delta(x-x_1)(y-y_1)$ is a sink term and represents the entrainment of larvae through the cooling station

a is equal to 1 if $L_{1i} < 5$ mm and equal to 0.2 if $L_{1i} > 7$ mm

d_ic_i is a sink term for the natural mortality

The tidal and diel behavior would be simulated in the same way as in the random walk model.

This method was not applied so a comparison can not be made with the random walk method. However, we could summarize the general disadvantages of this method as follows:

- the representation of source and sink terms is more easily modeled in the random walk model
- the computational effort increases linearly with n whereas in the random walk model the length of each larva is computed exactly without any additional computational effort

7 Model Simulations

7.1 Simulations

Three simulations were made using the 2-D random walk model. These simulated the fate of larvae hatched at Stations A, B, and C, respectively. The simulation time was equal to 131 days for each simulation covering the period between February 16, when larvae hatching starts, to June 26, when the last larva hatched has become a juvenile.

Particles were released over a two-month period (February 16 to April 26 which equals the hatching period) at a rate of 1 particle per timestep. The timestep was taken equal to 3h. Every particle represented the number or larvae born at that station in a 3-h period per 500 m^3. The birth rate distribution was calculated following the procedure described in Section 6 (Figure 11). Every particle was advected and diffused according to the algorithm described in Section 5. The diffusion parameter β for Niantic River was calculated to be equal to

$$\beta = \frac{T}{\pi^2} = \frac{12.4h}{\pi^2} = 1.25h \tag{29}$$

7.2 Input

The model requires the following input

1 Flow field data. These data are given from the circulation model TEA (Section 4).

2 The diffusion parameter β, the simulation time (131 days in this case), and the time over which particles are released which equals the time that larvae are spawned (70 days in this case).

3 Number of larvae/500 m^3 hatched every timestep, spatially averaged temperature values at every timestep, and data concerning larvae behavior.

7.3 Output

The output of every run includes the following information:

At each timestep the position of all particles released up to that time is recorded. In addition, at the end of the simulation the following information is summarized for each particle.

- #: number of the particle
- DOB: date of birth
- COHORT: Number of larvae/500 m^3 that are represented by the particle at the time the particle is released
- NSF: natural survival factor of the cohort at the end of the simulation (Equation (15))
- FSF: flushing survival factor. FSF can take the following value: 0 if the particle was flushed out of the domain or 1 if the particle was not flushed out
- ISF: intake survival factor. ISF can take the following values: 0 if the particle was entrained when the length of the larvae represented was less than 7 mm, 1 of the particle was not entrained, $(0.8)^n$ if the particle was n times entrained after the larvae reached the length of 7 mm.
- NENT: number of times particle has been entrained

- AGE: age in days of particle at the time when the program stopped tracking it
- LENGTH: length of the particle at the end of its simulation. LENGTH is less than 8 mm
- #LEFT: number of larvae a particle represents at the end of the simulation (i.e., the surviving fraction)
- DATE: last date of simulation for the particle
- LOC: location of particle when the program stopped tracking it

Figure 12 shows a page of the output file from the simulation of Station A.

After this list of information for every particle, cumulative statistics of larval fate are given. The length distribution is given for larvae entrained, flushed from the domain, and still in the domain at the end of the simulation. Also the number of larvae that died due to natural mortality and the number of larvae that metamorphosed to juvenile stage are given.

7.4 Comparison with Data

Verification of the model was attempted by comparing the simulated number and length distribution of entrained larvae with corresponding entrainment data provided by NUEL (personal communication).

Table 1a compares the number of larvae simulated to be entrained with the actual number calculated from measured data. The model simulates that about 1.5×10^6 larvae (hatched from all three stations combined) are entrained which is about 7% of the total of 22×10^6 larvae that were simulated to be hatched. However, data provided

#	DOB	COHORT	NSF	FSF	ISF	NENT	AGE	LENGTH	# LEFT	DATE	LOC	
31	18. FEBR	18.	11.90	0.03	0.00	1.00	0	34.13	4.1	0.000	24. MARCH 21.	-1576.20	-1036.63
#	DOB	COHORT	NSF	FSF	ISF	NENT	AGE	LENGTH	# LEFT	DATE	LOC	
32	18. FEBR	21.	11.90	0.04	1.00	0.00	0	30.25	3.9	0.000	21. MARCH 3.	2414.88	2445.98
#	DOB	COHORT	NSF	FSF	ISF	NENT	AGE	LENGTH	# LEFT	DATE	LOC	
33	19. FEBR	0.	11.90	0.07	0.00	1.00	0	25.50	3.7	0.000	16. MARCH 12.	-1191.69	-534.46
#	DOB	COHORT	NSF	FSF	ISF	NENT	AGE	LENGTH	# LEFT	DATE	LOC	
34	19. FEBR	3.	11.90	0.04	0.00	1.00	0	31.13	3.9	0.000	22. MARCH 6.	-1564.43	-1065.91
#	DOB	COHORT	NSF	FSF	ISF	NENT	AGE	LENGTH	# LEFT	DATE	LOC	
35	19. FEBR	6.	11.90	0.09	0.00	1.00	0	23.13	3.7	0.000	14. MARCH 9.	-1492.81	-923.02
#	DOB	COHORT	NSF	FSF	ISF	NENT	AGE	LENGTH	# LEFT	DATE	LOC	
36	19. FEBR	9.	11.90	0.01	1.00	1.00	0	80.38	8.0	0.087	10. MAY 18.	1274.22	6378.43
#	DOB	COHORT	NSF	FSF	ISF	NENT	AGE	LENGTH	# LEFT	DATE	LOC	
37	19. FEBR	12.	11.90	0.79	0.00	1.00	0	2.38	3.1	0.000	21. FEBR 21.	-1036.27	862.33
#	DOB	COHORT	NSF	FSF	ISF	NENT	AGE	LENGTH	# LEFT	DATE	LOC	
38	19. FEBR	15.	11.90	0.81	0.00	1.00	0	2.13	3.1	0.000	21. FEBR 18.	-2544.36	-2516.09
#	DOB	COHORT	NSF	FSF	ISF	NENT	AGE	LENGTH	# LEFT	DATE	LOC	
39	19. FEBR	18.	11.90	0.85	0.00	1.00	0	1.63	3.0	0.000	21. FEBR 9.	-1349.90	574.41
#	DOB	COHORT	NSF	FSF	ISF	NENT	AGE	LENGTH	# LEFT	DATE	LOC	
40	19. FEBR	21.	11.90	0.28	1.00	0.00	0	12.38	3.3	0.000	4. MARCH 6.	2429.71	2382.93
#	DOB	COHORT	NSF	FSF	ISF	NENT	AGE	LENGTH	# LEFT	DATE	LOC	
41	20. FEBR	0.	11.90	0.28	1.00	0.00	0	12.13	3.3	0.000	4. MARCH 3.	2561.23	2261.62
#	DOB	COHORT	NSF	FSF	ISF	NENT	AGE	LENGTH	# LEFT	DATE	LOC	
42	20. FEBR	3.	11.90	0.52	1.00	0.00	0	6.38	3.2	0.000	26. FEBR 12.	2594.93	2229.81
#	DOB	COHORT	NSF	FSF	ISF	NENT	AGE	LENGTH	# LEFT	DATE	LOC	
43	20. FEBR	6.	11.90	0.01	0.00	1.00	1	76.50	7.6	0.000	7. MAY 18.	11.64	-3018.74

Figure 12 Model output

Table 1a

Comparison of Seasonal Total of Entrained Larvae Simulated by the Model (as a Function of Station where Hatching Occurred) versus Measured at Intake from NUEL

Simulation	Total number ($\times 10^6$)	Percent of larvae hatched
Sta A	0.30	5.2
Sta B	0.80	6.0
Sta C	0.38	8.8
total	1.48	6.7
Measurement	98.0	450.

Table 1b

Comparison of Length Distribution of Entrained Larvae Simulated by Model (as a Function of Station where Hatching Occurred) versus Mesaured Data from NUEL (percent)

	length range in mm					
Simulation	3-4	4-5	5-6	6-7	7-8	total
Sta A	85.2	5.4	7.1	2.2	0.1	100
Sta B	93.5	2.8	2.2	1.6	0.1	100
Sta C	94.6	3.0	1.2	1.1	0.1	100
ave.	91.7	3.5	3.0	1.7	0.1	100
Measurement	17.8	18.6	24.3	23.1	16.2	100

by NUEL, 1988 (p 184) indicate that an annual average of about 98 × 10^6 larvae was entrained during the years 1984-87 which is nearly two orders of magnitude greater than the number simulated and 4.5 times greater than the number of hatched larvae input to the model! Clearly we are not simulating enough larvae in the system.

Table 1b shows simulated and observed length distributions. It is clear that the two length distributions are very different: the model simulations for year 1984-87 indicate that about 92% of the entrained larvae have a length between 3 mm and 4 mm, while the data from NUEL show only about 18% of larvae entrained have a length between 3 mm and 4 mm. There is also a corresponding discrepancy (not shown) in the times of peak entrainment with model times being much quicker than observed times. However, this latter discrepancy is not surprising. Assuming that we are using a valid growth relationship, we should expect to see a strong correlation between young and short larvae. And, indeed, the agreement between dates of peak abundance and mean larval length is quite good. It should also be noted that, while the simulated distribution of entrained larvae is strongly skewed to the shorter lengths (compared with data), the actual number of short larvae is still considerably less than observed. For example, the simulations indicate that about 1.4 × 10^6 larvae were entrained in the interval of 3-4 mm (92% of 1.5 × 10^6 total larvae entrained) while the data indicate that about 18 × 10^6 larvae were entrained (18% of 98 × 10^6 total larvae entrained).

In summary, the model is indicating that far too few larvae are being entrained and that the larvae that are being entrained are generally shorter (younger) than those observed.

8 Analysis

There are several hypotheses that could explain, in whole or in part, one or both of the two discrepancies:

1) The input hatching rates are too small

2) The input larval mortality rates are too small

3) Larval residence times within Niantic River are too short due to either
   a) overestimation of hydrodynamic flushing rates, or
   b) underestimation of larval retention mechanisms (behavior, etc.)

4) The model is underestimating the percentage of larvae within the bay that are being entrained

5) Larvae are being imported from outside the Niantic River area

Each hypothesis is discussed briefly in turn.

8.1 Hatching Rates

The data indicate that almost five times more larvae are being entrained than we are simulating to be hatched. Clearly the source of larvae in the model is too small, and one explanation is that too few larvae are being simulated to be hatched. It is estimated that 15-20 × 10^9 eggs were spawned during each of the years 1984-87 (NUEL Annual Report, 1989, p 267). Assuming a 10% egg hatching rate (NUEL personal communication), the number of larvae hatched should be 1500-2000 × 10^6 rather than 22 × 10^6 which we calculate from the density of yolk-sac larvae. It seems possible to us that, because they are negatively buoyant, the yolk-sac larvae reside primarily near the bottom, and hence that they are undersampled with the bongo sampling system.

Note that merely increasing the number of larvae hatched would help explain the discrepancy between the simulated and observed number of entrained larvae, but would not, by itself, explain the discrepancy in the length distribution. However, if the hatching rate were underestimated *because the yolk-sac larvae reside near the bottom*, this could also help explain the length distribution. This is because larvae residing near the bottom, where currents are smaller, would be more likely to be retained in the river.

To explore this possibility, *it is recommended that more detailed surveying (in the vertical) be undertaken when larvae are next sampled.*

8.2 Mortality Rates

Larval mortality is known to be a complicated function of age, density, and other factors so it is possible that the mortality rates (see Section 6.4) are too high. Lower mortality would allow older larvae to survive, thus increasing the total number of entrained larvae and shifting the entrainment distribution to longer lengths. Table 2a shows the total number of larvae entrained and Table 2b shows the length distribution for model simulations that assumed *zero mortality rate.* Compared with Table 1a, the total number of entrained larvae has increased by a factor of 3.5 (5.2×10^6 vs. 1.5×10^6) but is still much smaller than the data indicate. And, compared with Table 1b, the simulated length distribution is more uniform but still there is a maximum (59.8%) at the lower lengths (3–4 mm). From the above *we can conclude that a discrepancy in the mortality rates does not explain alone the difference in either the total number or the length distribution of entrained larvae.*

Table 2a

Seasonal Total of Entrained Larvae Simulated by the Model
(as a Function of Station where Hatching Occurred)
assuming *zero* mortality rate

Station	Total number ($\times 10^6$)	Percent of larvae hatched
A	1.51	25.7
B	2.73	20.4
C	0.99	23.0
total	5.23	21.0

Table 2b

Length Distribution of Entrained Larvae Simulated by the Model
(as a Function of Station where Hatching Occurred)
assuming *zero* mortality rate (percent)

	length range in mm					
Station	3-4	4-5	5-6	6-7	7-8	total
A	44.4	12.3	27.2	14.8	1.3	100
B	66.2	11.4	9.4	11.2	1.8	100
C	63.8	14.7	7.9	9.3	4.3	100
average	59.8	12.8	13.5	11.5	2.5	100

8.3 Larval Residence Times

The third hypothesis is that larval residence times are being underestimated due either to overestimation of hydrodynamic flushing or misrepresentation of larval transport, in comparison with that of passive particles. Increasing larval residence times would allow the larvae to age, hence increasing their length distribution. However, all else equal, their greater age would result in greater mortality, thus *decreasing* the total number of entrained larvae. Thus *increasing residence time, by itself, can not completely explain the discrepancy between model and data.*

Regarding hydrodynamic flushing, we note that the random walk model was calibrated to Ketchum's tidal mixing model. This model is an idealized 1-D model that is based on the assumption of complete mixing within every volume segment. It requires validation for complex real estuary mixing. Accordingly, *we suggested that a dye study be conducted to explore hydrodynamic flushing.* This was done and the results of the study, along with an analysis of salinity data, are discussed in Section 9.

Regarding larval transport, it is possible that we are underestimating the role of vertical migration or other mechanisms that would allow larvae to be retained within the estuary. As mentioned in Section 8.1, younger larvae may tend to reside near the bottom simply because their specific gravity exceeds one. Because of slower water velocities near the bottom, they would require longer times to be flushed from the river. And, as mentioned earlier, if their residence near the bottom results in their being undersampled, this could explain both the low number *and* the short length distribution of entrained larvae.

Support for this hypothesis is provided by examination of the dates of peak abundance of larvae sampled in the river (Stations A, B, and C) and in the bay. These are discussed in Section 9 following presentation of the hydrodynamic flushing rates.

To pursue this further *we recommend that methods be explored to improve the vertical resolution in larval sampling.*

8.4 Entrainment within the Bay

A fourth hypothesis is that, because of uncertainty in hydrodynamic model formulation, boundary conditions, dispersion coefficients, etc., we are underestimating the fraction of larvae within Niantic Bay that are being entrained by the plant. Increasing this fraction would increase the total number of entrained larvae, but clearly not by as much as the data indicate. (Even if 100% of the larvae were entrained, and there were zero mortality, the number of entrained larvae simulated would still be less than the number observed by a factor of five.) Nonetheless, it is important that the hydrodynamic calculations within the bay be verified and hence *we suggested that a second dye study be conducted.* This was done and the results are presented in Section 9.

8.5 Larval Import

A final hypothesis is that larvae are being imported from different spawning areas (e.g., Connecticut River). Because these areas are further away, the time of travel would be longer, which could help explain why observed entrainment times exceed simulated times. It would obviously also explain the underestimation of entrained larvae.

The import hypothesis is supported by considering the following mass balance equation for larvae in the bay:

$$\frac{d}{dt}c_{bay} = (c_r - c_{bay})\frac{P}{\forall T} - kc_{bay} - \frac{Q_0 c_{bay}}{\forall} \pm s/s \qquad (30)$$

where

c_{bay} = density of larvae in bay

c_r = density of larvae in river

P = tidal prism volume of river

V = volume of bay

T = tidal period

k = natural mortality rate

Q_0 = condenser cooling water flow rate

s/s = source(+)/sink(-) for larvae from/to Long Island Sound

The s/s term has been calculated as the residual term needed to close Equation (30) using data provided by NUEL for the remaining terms. Table 3 summarizes these calculations for the years 1984-88. It is consistently seen that for early times s is a sink term, while for later times s is a source. A reasonable explanation for the source is that, at later times, larvae are imported. However, the magnitude of the source is not sufficient to explain the magnitude by which the model is underrepresenting entrainment. And a further problem that appears in this interpretation is the large magnitude of the sink term at early times. It is possible that the spatial distribution of the larvae in both the vertical and the horizontal is non-uniform, making the above mass balance (which is based on measured concentrations at single points in the river and the bay) very approximate. Again, *we recommend that the spatial resolution be increased in future larval sampling.*

9 Tracer Studies

In order to pursue the two hypotheses that are related to hydrodynamics (3a and 4), a pair of dye studies was conducted. The purpose of the first study, conducted in Niantic River, was to measure the flushing time and hence calibrate the random walk

Table 3

Evaluation of Source/Sink Terms in Niantic Bay Larval Balance, 1984-88

10-day group*	s/s term (number/500m³·10d) 1984	1985	1986	1987	1988
Feb 15 - Feb 24	-255	-2	-167	-428	-1935
Feb 25 - Mar 6	-430	-372	-206	-801	-3639
Mar 7 - Mar 16	-598	-2001	-235	-1018	-3457
Mar 17 - Mar 26	-679	-2143	-251	-937	-2191
Mar 27 - Apr 5	-459	-834	-187	-445	-885
Apr 6 - Apr 15	47	110	151	120	8
Apr 16 - Apr 25	399	446	437	342	410
Apr 26 - May 5	418	459	381	297	480
May 6 - May 15	262	363	193	184	403
May 16 - May 25	94	257	44	94	293
May 26 - Jun 4	-20	172	-38	41	198
Jun 5 - Jun 14	-81	111	-73	14	128
Jun 15 - Jun 24	-104	70	-83	2	81

*Feb 29 ignored in 1984 and 1988

transport model of the estuary. This flushing time could then be compared to the flushing time resulting from Ketchum's model, thus testing hypothesis 3a. The second dye study was conducted to estimate transport between the estuary mouth and the intake, addressing hypothesis 4.

9.1 Dye Study 1

The motivation for the first study was the estimation of the estuary flushing time. As mentioned above, the length distribution of entrained larvae that resulted from the model simulation was different from the actual data. The random walk transport model used for these simulations was calibrated using an idealized model for tidal mixing in an estuary. With data from a dye study, the model could be calibrated from field data.

Dye Study 1 was conducted from November 16 through December 15, 1988. During this period 359 lbs of 20% Rhodamine WT dye solution was injected from a location near the head of the river (Figure 3). Hence dye was injected at an average rate of 0.0468 kg of pure dye per hour. The following data were measured:

- Continuous concentrations during this period at the Mijoy Dock (Figure 13) and the Millstone Quarry

- Transverse concentrations across the river at a depth of 2 ft during high slack and low slack) on December 15, 1988. The locations of the transects are shown in Figures 14 and 15 respectively and the transect average concentrations are shown in Table 4.

- Vertical profiles of concentration at Stations 1 through 11 (see Figures 14, 15) at high slack (Figure 16) and low slack (Figure 17) on December 15, 1988

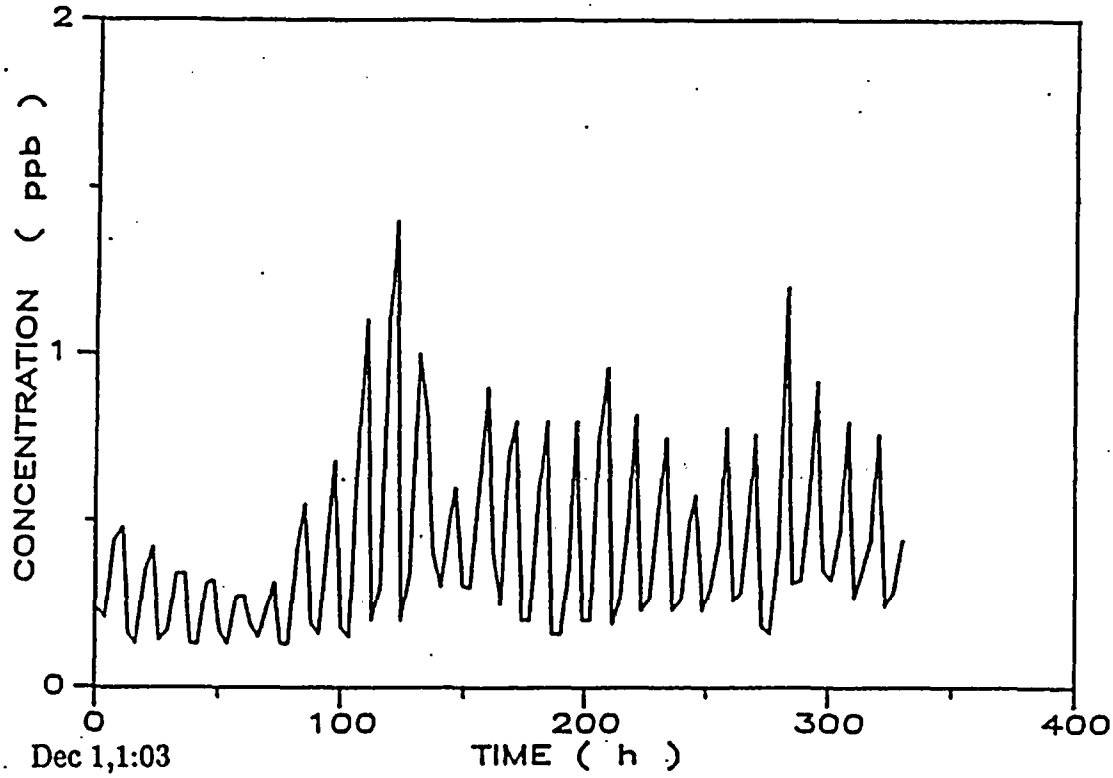

Figure 13 Dye concentrations at the Mijoy Dock in the period from December 1 to December 15

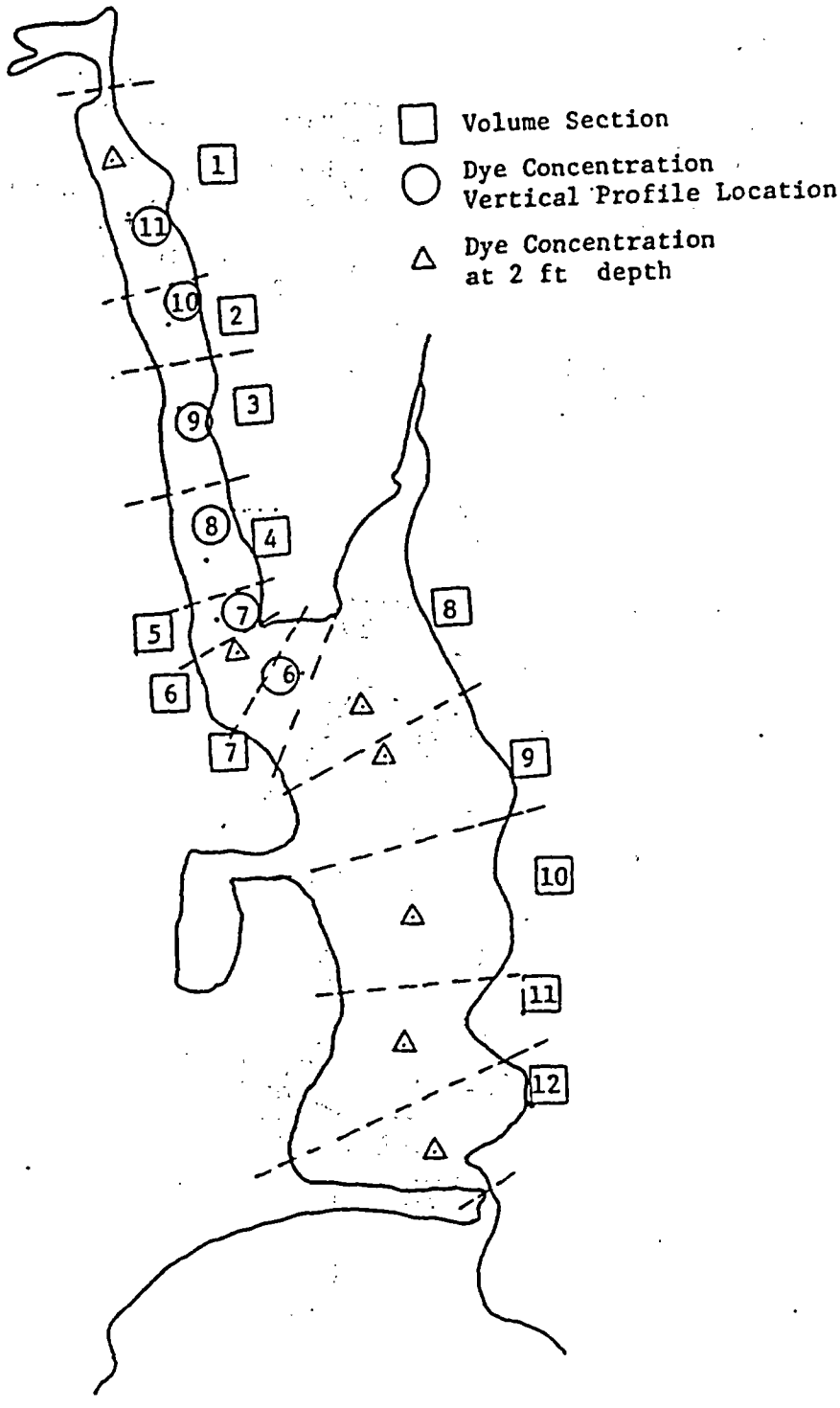

Figure 14 Locations of transverse and vertical concentration measurements at high slack on December 15, 1988

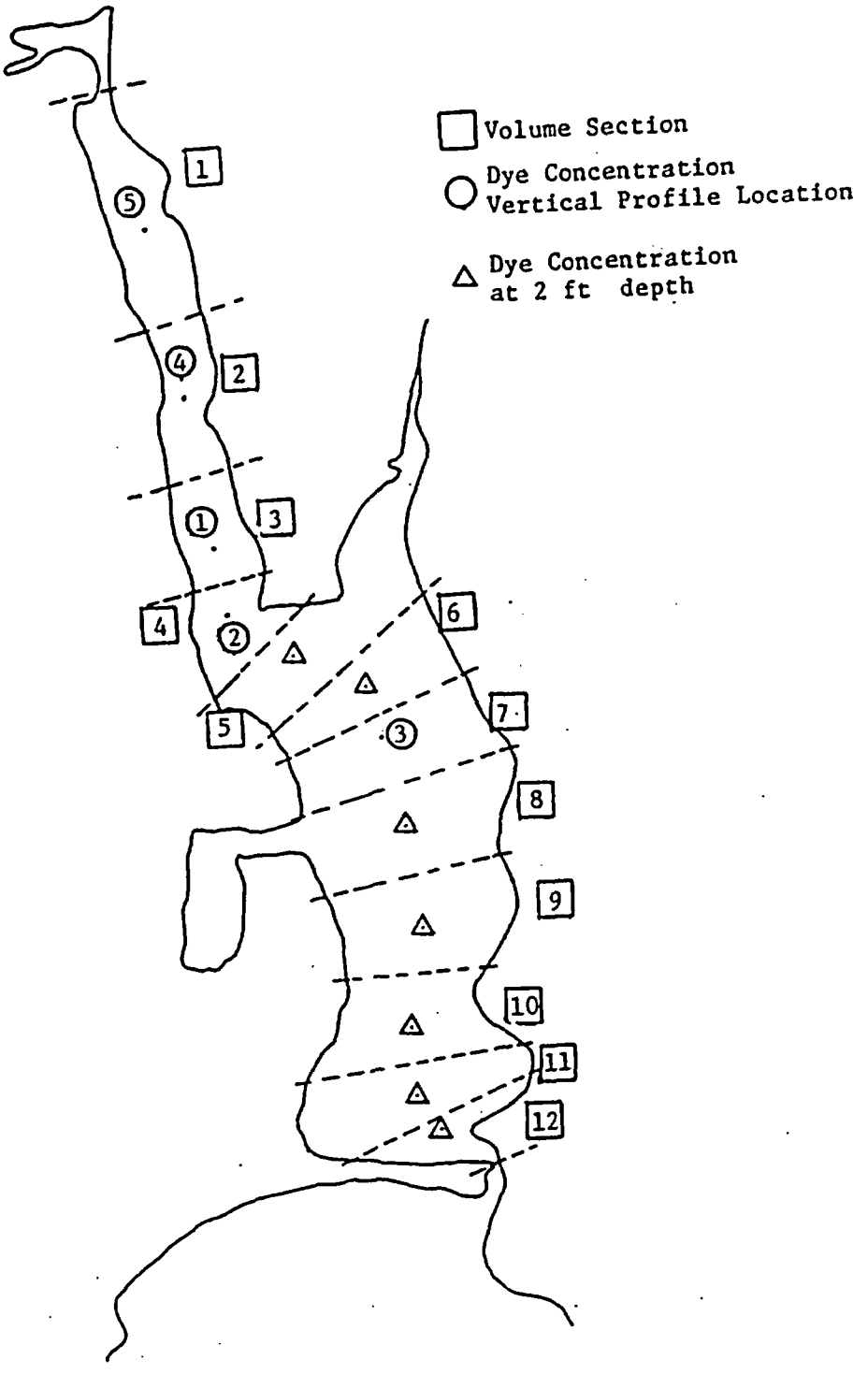

Figure 15 Locations of transverse and vertical concentration measurements at low slack on December 15, 1988

Table 4

Averages and Standard Deviations of Dye Concentration Measured along Transects Shown In Figures 14 and 15

High Tide

Volume Section	Concentration (ppb)
1	0.58 ± .15
6	0.45 ± .06
8	0.36 ± .05
9	0.36 ± .07
10	0.34 ± .05
11	0.22 ± .08
12	0.19 ± .04

Low Tide

Volume Section	Concentration (ppb)
5	0.33 ± .07
6	0.38 ± .04
8	0.30 ± .04
9	0.28 ± .07
10	0.22 ± .04
11	0.18 ± .02
12	0.19 ± .04

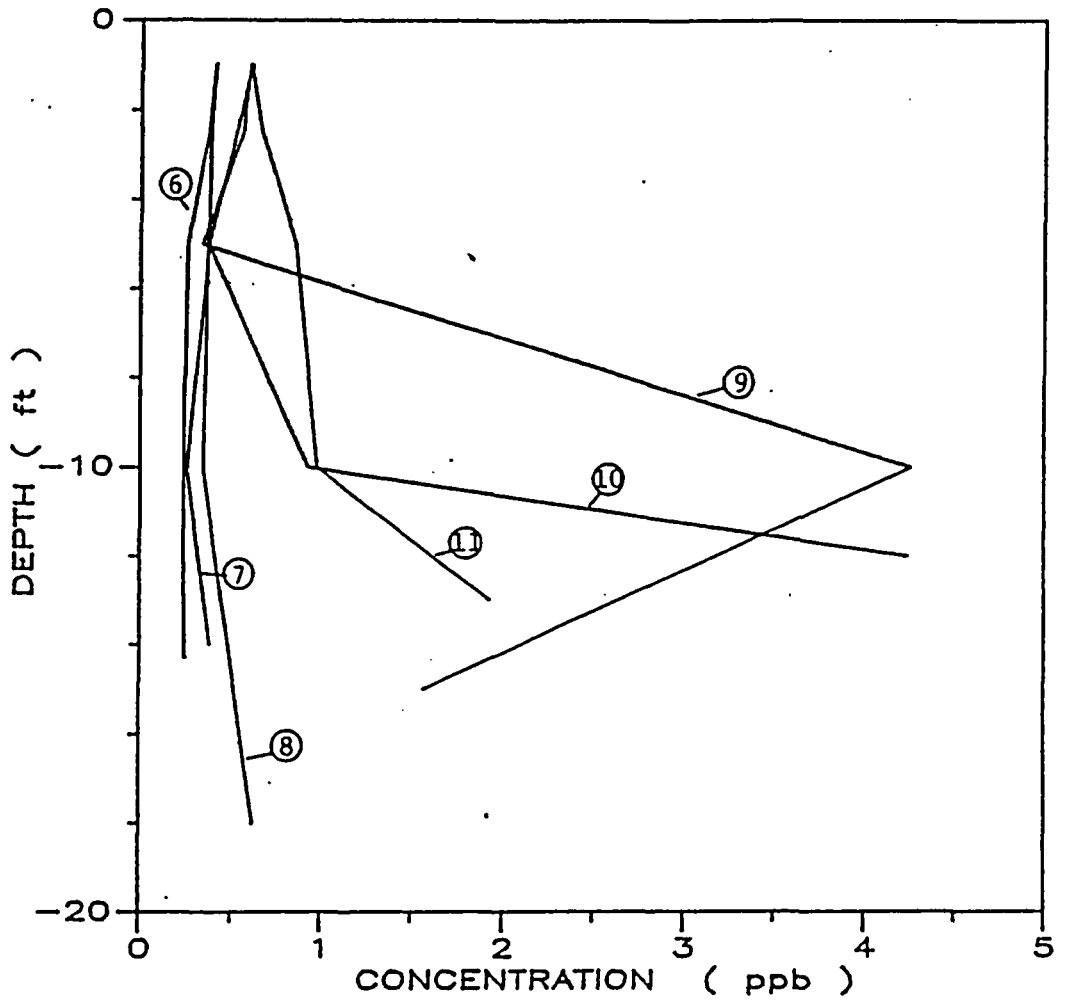

Figure 16 Vertical profiles of concentration at high slack on December 15, 1988

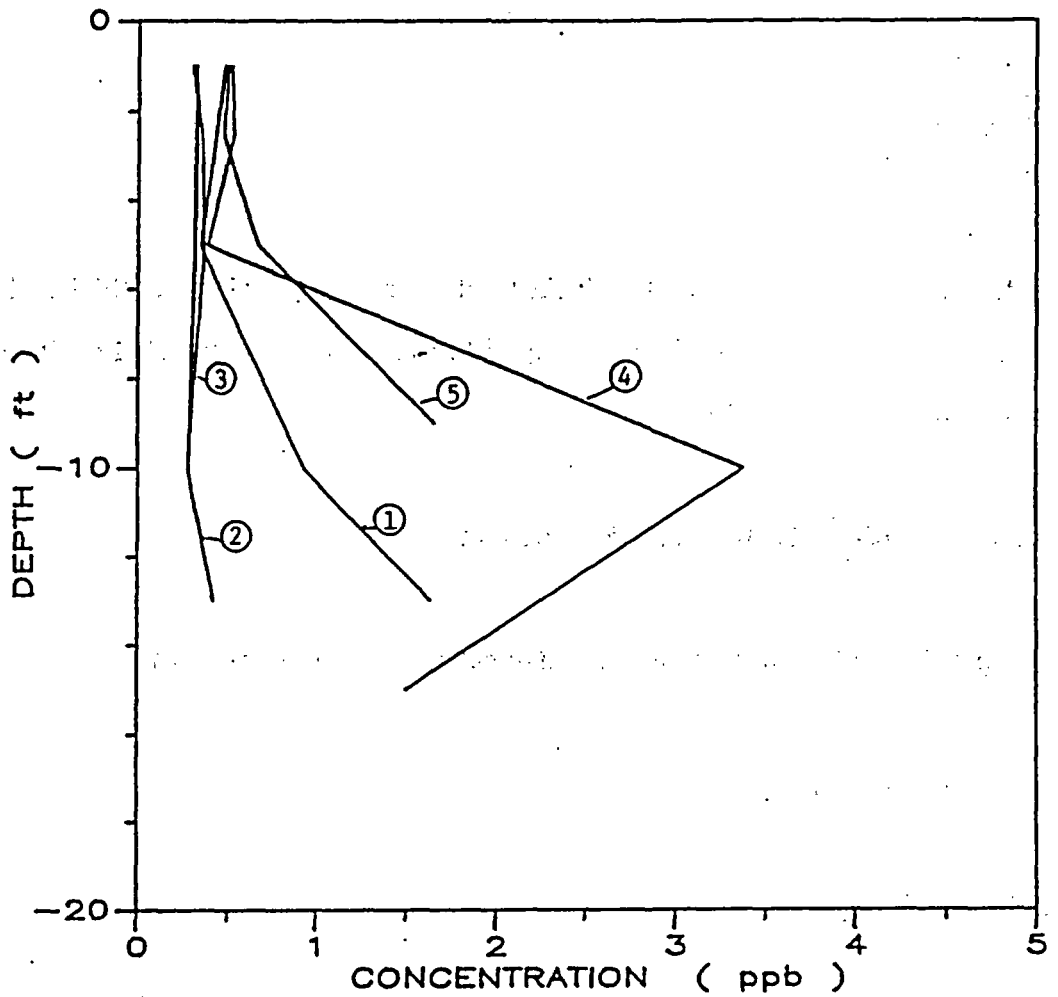

Figure 17 Vertical profiles of concentration at low slack on December 15, 1988

Figure 13 shows dye concentrations at Mijoy dock for the period between December 1, 1988, and December 14, 1988. From this figure we can assume that quasi-steady-state conditions were reached after December 5, 1988. As a check, we can perform the following mass balance. If we designate as c the dye concentration at Mijoy and Q the flow at Mijoy then the integral

$$\int_0^T Q \cdot c \cdot dt \tag{31}$$

represents the net mean of dye that is flushed out of the river during one tidal cycle T. If dye is conservative this mass should be equal to the mass of dye injected during one tidal cycle m_{in} which is equal to

$$m_{in} = 0.0468 \frac{kg}{h} \cdot 12.4h = 0.58 \text{ kg pure dye} \tag{32}$$

We approximate the time variation of dye concentration at Mijoy as

$$c = \bar{c} + c_{max}[\sin(\omega t - \phi)] \tag{33}$$

and the flow at Mijoy as

$$Q = Q_{max} \cdot \sin\omega t \tag{34}$$

The value of Q_{max} is found by integrating Equation (34) over the duration of ebb flow and setting the result equal to the average tidal prism. The unknown parameters of Equation (33) are determined by a least squares regression analysis between the theoretical concentration variation described by Equation (33) and the observed

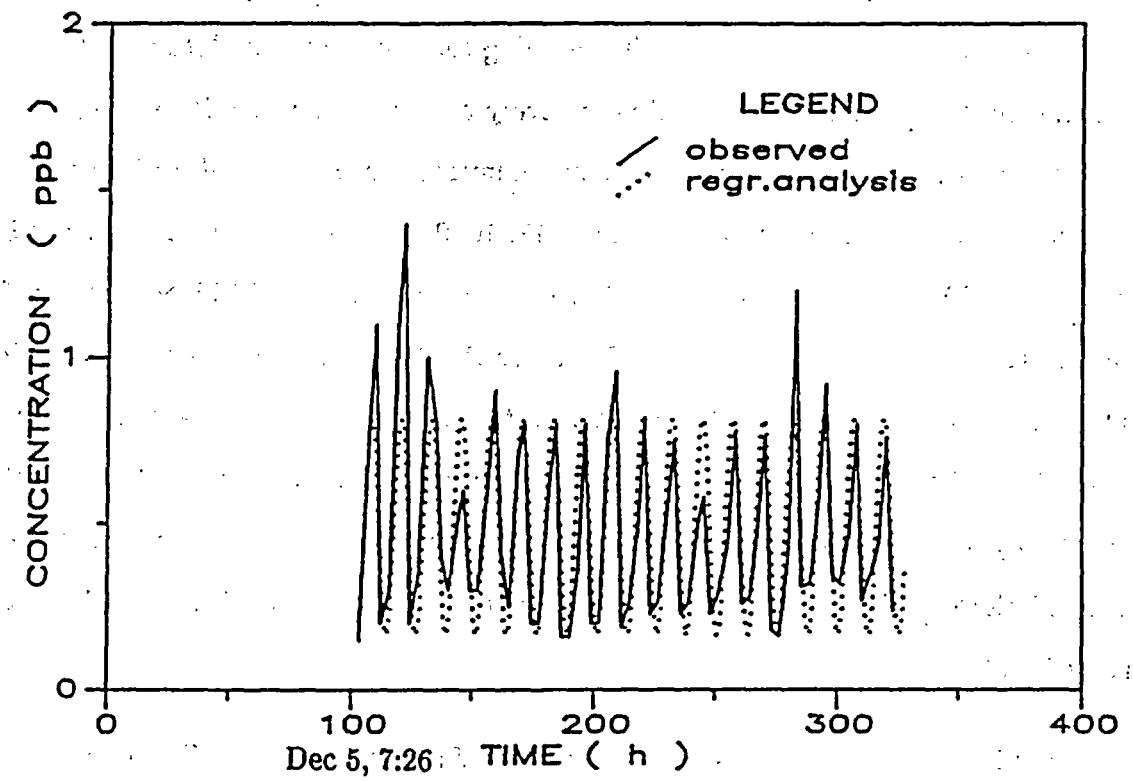

Figure 18 Comparison between steady-state concentration data at Mijoy Dock and results from regression analysis

If we designate the dye concentration at any given location in the estuary as c, the mass of dye in the estuary is given by the integral

$$V_d = \int c \, dV \tag{37}$$

where the integral is taken over the entire volume of the estuary.

The following remarks can be made regarding the concentration data used to evaluate Equation (37). Concentrations at every cross section show little variation which means that we have complete transverse mixing. In the vertical profiles at sections upstream from Sandy Pt. (Sections 11, 10, 9, 8 for high slack and Sections 5, 4, 1 for low slack), near-bottom concentrations are up to a factor of 10 higher than surface concentrations. This probably occurred because the dye is negatively buoyant, so close to the injection point it fell to the bottom. In the sections that are located south of Sandy Point (i.e., Sections 7, 6 for high slack (Figure 14) and Sections 2, 3 for low slack (Figure 15)) concentration is essentially vertically uniform. So we conclude that we have complete vertical mixing in the lower part of the estuary that is located beneath Sandy Point.

The following technique was used to evaluate V_d (Equation 37). The river was divided into n sections, corresponding to the measured concentrations, and at every section i the integrated concentration was approximated as $\overline{c_i}V_i$. Different assumptions were made concerning the segment average concentration $\overline{c_i}$ upstream and downstream from Sandy Pt. Downstream the segments were defined by the location of the lateral transects; the concentrations measured at 2-ft intervals were averaged laterally and assumed to be uniform over depth. Upstream from Sandy Pt. the segments were defined by the vertical profile; concentrations were averaged over the depth and were assumed to be uniform laterally. Figures 14 and 15 show the sections for high and low

slack respectively. V_d was then found by summing the mass from each segment and the flushing time was calculated using Equation (37).

Using this method the flushing time for the low slack data was 2.6 d, the flushing time for the high slack data was 3 d, and the mean was about 2.8 d.

9.2 Salinity

Vertical salinity profiles (Figure 19) at locations indicated in Figure 20 were taken at high tide on December 15. Salinity can be used as an alternative to dye for estimating flushing times of estuaries. If we designate the total river inflow rate by R and the total freshwater volume of the estuary by V_f, the flushing time is given by analogy with Eq. (36) as

$$t_{res} = \frac{V_f}{R} \tag{38}$$

where R is the discharge from Lattimer Brook. V_f in turn is evaluated by spatial integration of the local freshness, defined as

$$f = \frac{\sigma - s}{\sigma} \tag{39}$$

where σ is the "ocean" salinity and is the total salinity. In analogy with Eq. (37),

$$V_f = \int f d\forall \tag{40}$$

R was determined from discharge rates for Pendleton Brook for the period November - December 1988 (Table 5). Using linear regression, the discharge rates of

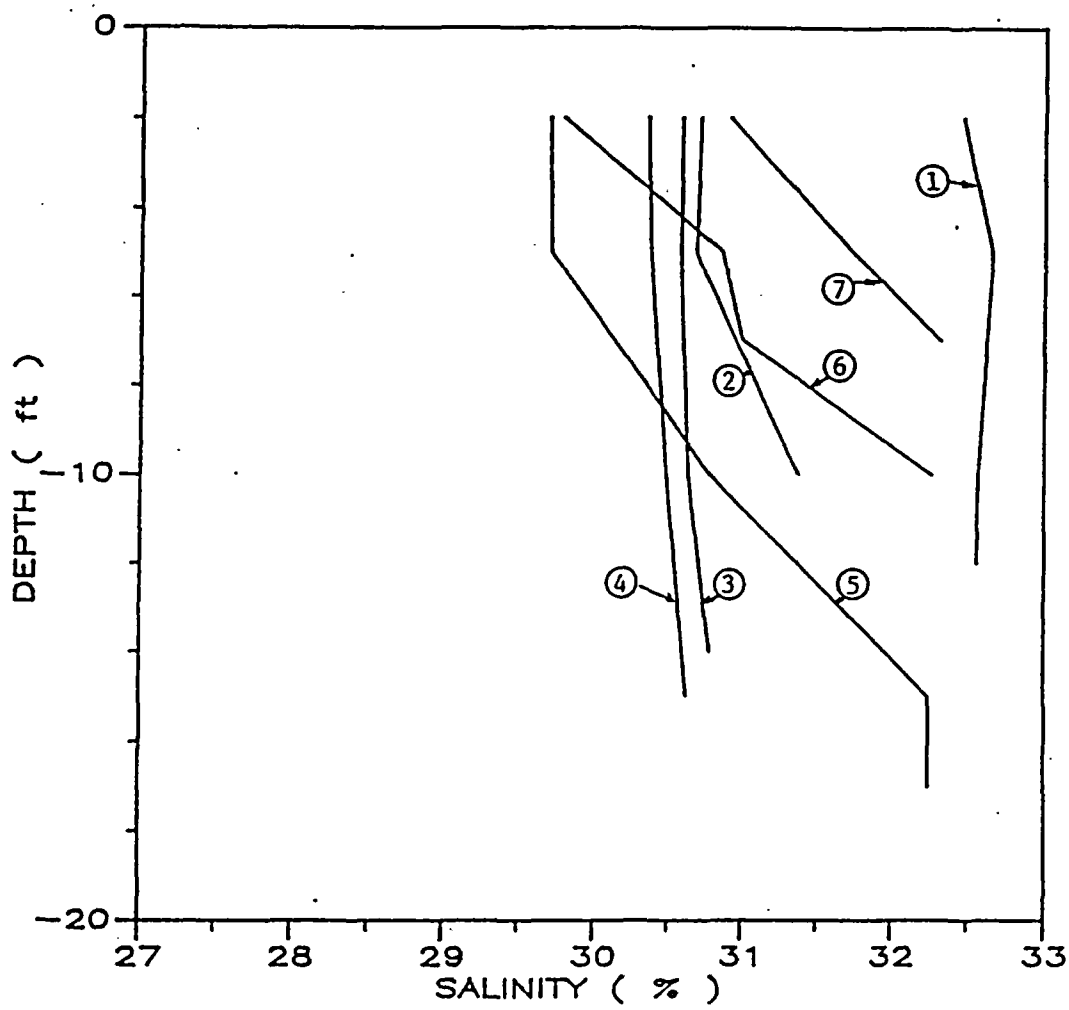

Figure 19 Vertical profiles of salinity at high slack on December 15, 1988

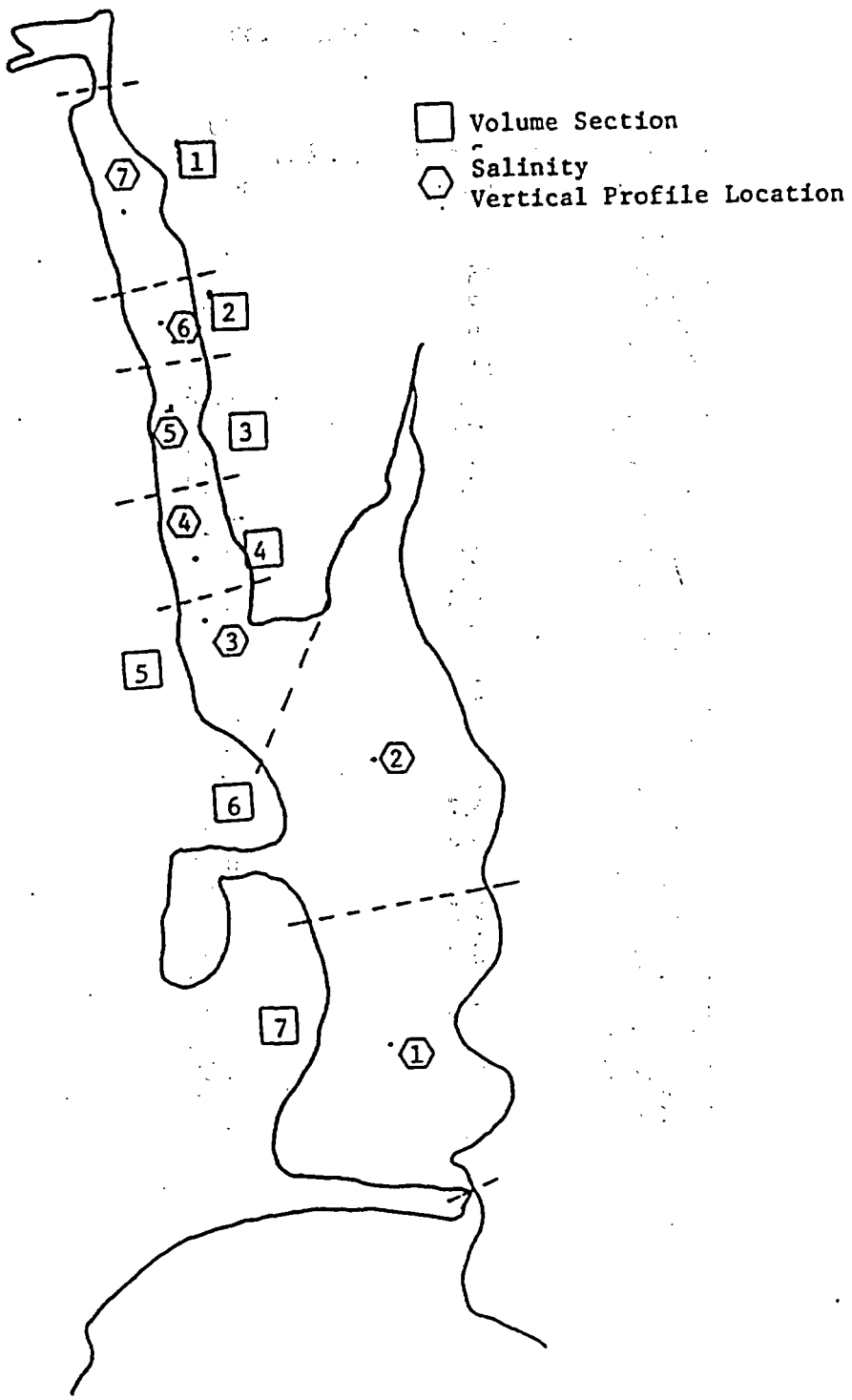

Figure 20 Locations of salinity measurements at high slack on December 15, 1988

Table 5

Flow Data for Latimer Brook

Date	Q Pendleton Brook (cfs)	Q Lattimer Brook (m^3/s)
12/1/88	18	1.53
12/2/88	15	1.27
12/3/88	13	1.11
12/4/88	12	1.02
12/5/88	11	0.94
12/6/88	9.9	0.85
12/7/88	9.6	0.82
12/8/88	9.1	0.78
12/9/88	8.4	0.72
12/10/88	7.7	0.67
12/11/88	7.0	0.61
12/12/88	5.9	0.52
12/13/88	5.9	0.52
12/14/88	12	1.02
12/15/88	11	0.94
12/16/88	8.7	0.75
12/17/88	7.1	0.62
12/18/88	6.2	0.54
12/19/88	5.8	0.51
12/20/88	5.7	0.50
12/21/88	5.8	0.51
12/22/88	5.8	0.51
12/23/88	5.8	0.51
12/24/88	5.8	0.51
12/25/88	5.8	0.51
12/26/88	5.9	0.52
12/27/88	6.0	0.52
12/28/88	6.0	0.52
12/29/88	6.0	0.52
12/30/88	6.0	0.52
12/31/88	6.1	0.53

Lattimer Brook are related to the discharge rates of Pendleton Brook by (NUEL, personal communication):

$$CFS_{lattimer} = 0.795 + 2.948 \cdot CFS_{pendleton} \tag{41}$$

The flushing time was calculated by dividing the estuary horizontally into seven sections (Figure 20) and the volume V_i of each section was calculated. At each section and depth, values of freshness were computed. The ocean salinity was taken as the salinity of Station 1 (Figure 19). Values at different depths were then averaged to determine a section-average freshness, f_i. The value of R was based on the flow averaged over n days preceding measured salinity. Table 6 shows the sensitivity of the flushing time to the value of n. We see that the values of the flushing time are between 3.9 d and 5.3 d which is a little higher than the flushing time of 2.8 d we get from Dye Study 1.

Flushing times were also determined from earlier salinity data at Stations A, B, C, and Niantic Bay for the period Feb.-April 1985, 86, 87, 88. Salinity data are given at surface, middepth, and bottom, although for some sections the middepth data are missing. The value of R was taken equal to the averaged flow over the week preceding measured salinity. In Table 7 the values of flushing times for different days are shown. We can see that the values of the flushing time are between 1.4 d and 4.5 d which is also consistent with the flushing time of 2.8 d that we get from Dye Study 1.

9.3 Comparison between Flushing Time Estimated from Tracer Studies and Model MILL

From Sections 9.1 and 9.2 we see that the observed flushing times using either dye or salinity are considerably smaller than the theoretical time based on Ketchum's model

Table 6

Sensitivity of Flushing Time on the Number of Days n Used to Average Flow

n (days)	flushing time (days)
1	4.1
2	3.9
3	4.7
5	5.2
6	5.3
7	5.2

Table 7

Flushing Times Using Salinity Data

date	discharge Pendelton Brook (cfs)	discharge R Latimer Brook ($10^3 m^3/d$)	flushing time (days)
21 Mar 85	10.79	79.8	4.4
28 Mar 85	6.87	51.5	3.7
4 Apr 85	7.79	58.1	4.5
12 Apr 85	6.21	46.8	2.1
18 Apr 85	4.89	37.2	5.9
6 Mar 86	8.53	63.5	1.4
20 Mar 86	29.14	21.2	1.5
3 Apr 86	10.17	75.3	3.2
14 Apr 86	8.67	66.6	1.8
24 Apr 86	6.55	49.2	4.5
12 Mar 87	15.14	111.2	1.9
26 Mar 87	7.37	55.1	3.7
7 Apr 87	50.14	363.6	3.0
16 Apr 87	21.00	153.4	2.4
3 Mar 88	9.03	67.1	3.6
17 Mar 88	8.4	62.6	3.6
11 Apr 88	10.81	79.9	3.5
21 Apr 88	6.67	50.1	4.5

(and hence the time to which the model MILL has been calibrated). This may be due to vertical stratification, uneven bathymetry (resulting in tidal pumping), or other effects that allow mixing to take place over distances larger than a theoretically computed tidal excursion. The effect is that the longitudinal dispersion coefficient D_{xx}, and hence the model mixing parameter β should be *increased* in order to match the observed flushing rates. All else equal, this would *decrease* the average time it takes for larvae to be entrained at the intake, leading to a greater discrepancy between the simulated and observed distribution of entrained larval length. As mentioned in Section 7 the majority (91.7%) of the larvae entrained according to the model simulation had a length between 3-4 mm while the data showed that only 12.4% of larvae entrained had a similar length.

The dye study and the theoretical hydrodynamic flushing calculations pertain to passive particles that follow the flow. Larvae, of course, may be transported differently. (The behavior introduced in the model is one example.) It is difficult to measure the residence time of larvae because they are not easily "marked." However, we can infer their approximate residence time by examining the dates of peak abundance observed at different stations.

Table 8 shows dates of peak abundance of winter flounder larvae for the years 1983-1988 at the three Niantic River Stations (A, B, and C) and for Niantic Bay. These peak abundances suggest the following average residence times

between Station A and B	5.7 d
between Station B and C	14.5 d
between Station C and Niantic Bay	24.5 d

Table 8

Peak Abundances of Winter Flounder Larvae
(from NUEL, personal communication)

Estimated dates of peak abundance of winter flounder larvae at the three Niantic River stations (A, B, and C) and for Niantic Bay (entrainmenat and mid-Niantic Bay combined).

Year	Sta A	Sta B	Sta C	Niantic Bay
1983	Mar 6	Mar 20	Apr 9	Apr 17
1984	Mar 4	Mar 12	Apr 4	Apr 22
1985	Mar 9	Mar 14	Mar 19	Apr 12
1986	Feb 26	Feb 28	Apr 1	Apr 23
1987	Mar 8	Mar 9	Mar 17	Apr 17
1988	Feb 29	Mar 5	Mar 5	Apr 18

According to this the average residence time of larvae in Niantic River is equal to 45 d which is about fifteen times larger than the flushing time of the estuary obtained from the dye study and about three times as large as the time simulated in the model (15 d). The facts that more larvae were entrained than would be expected based on hatching rates, plus the considerably larger residence time of larvae relative to dye, could both be explained if it were determined that the younger as well as the older larvae were found predominantly near the bottom, where they might be undersampled and transported more slowly than dissolved dye.

9.4 Dye Study 2

Dye Study 2 was conducted from January 11-17, 1989. The motivation for the second study was to better understand the residence time of larvae between the mouth of the Niantic River and the intake as well as to measure the percentage entrainment. In this regard, dye studies had been done in the past. Specifically Ocean Systems, Inc., conducted four dye experiments during June and July 1975 and a fifth study in March 1976. Figure 3 shows the locations of these studies. The purpose of these studies was to verify the previous concentration models by comparing the percentage of dye entrained to the percentage of larvae entrained.

During ebb tide (1300 to 1700 hrs) on January 11 307 lbs of 20% Rhodamine WT dye solution were injected in the vicinity of the NRRR Bridge (Figure 3). Fluorometers with strip chart recorders measured dye concentrations at the station quarry and at Mijoy Dock. Concentration measurement started one day before the dye release (January 10, 11:20) and continued for 6.5 consecutive days (until January 15, 22:18). During this time the station experienced full operation from all three units.

The concentration of dye at the quarry as a function of time is shown in Figure 21. Time 0 corresponds to the time of the dye release. The background concentration was estimated from measurements on the day before the dye release. According to these data the background concentration changes as a function of the tidal cycle, and ranged from 0 to 0.18 ppb, with an average of 0.12 ppb. The percent of injected dye that passes through the intake is calculated as

$$\frac{Q_0 \int_0^{t_{end}} (c-c_b)dt}{M_0} \cdot \frac{10^{-6}kg}{m^3\text{-ppb}} \cdot 100\% \qquad (42)$$

where Q_0 the condenser flow rate = 118 m^3/s, c_b is the background concentration, t_{end} is the end of the survey (6.5 d), and M_0 is the mass of pure dye injected = 28 kg. Using our best estimate of c_b = 0.12 ppb, the percentage recovery is 20.6%. A sensitivity analysis was made in order to estimate the relationship between the background concentration and the amount of dye entrained. The results are shown in Table 9. It can be concluded from this table that a variation in the background concentration between 10% and 15% results in a variation in the percentage of dye passing through the intake of between 25% and 15%.

The results of the second dye experiment were compared with Study No. 5 conducted by Ocean Systems, Inc., on March, 11 1976 (Ocean Systems, Inc., 1976). The earlier study involved 25.9 kg of pure dye discharged over 12.5 hours at the location shown in Figure 3. Concentrations were measured at Mijoy dock and the quarry for only three days after the dye release because of pump and power supply failures. Assuming a plant flow of 61 m^3/s (only two units were operating at that time) OSI calculated that 6.8% of the dye was entrained. Taking into account that: 1) three units were operating (118 m^3/s) during the second dye experiment and

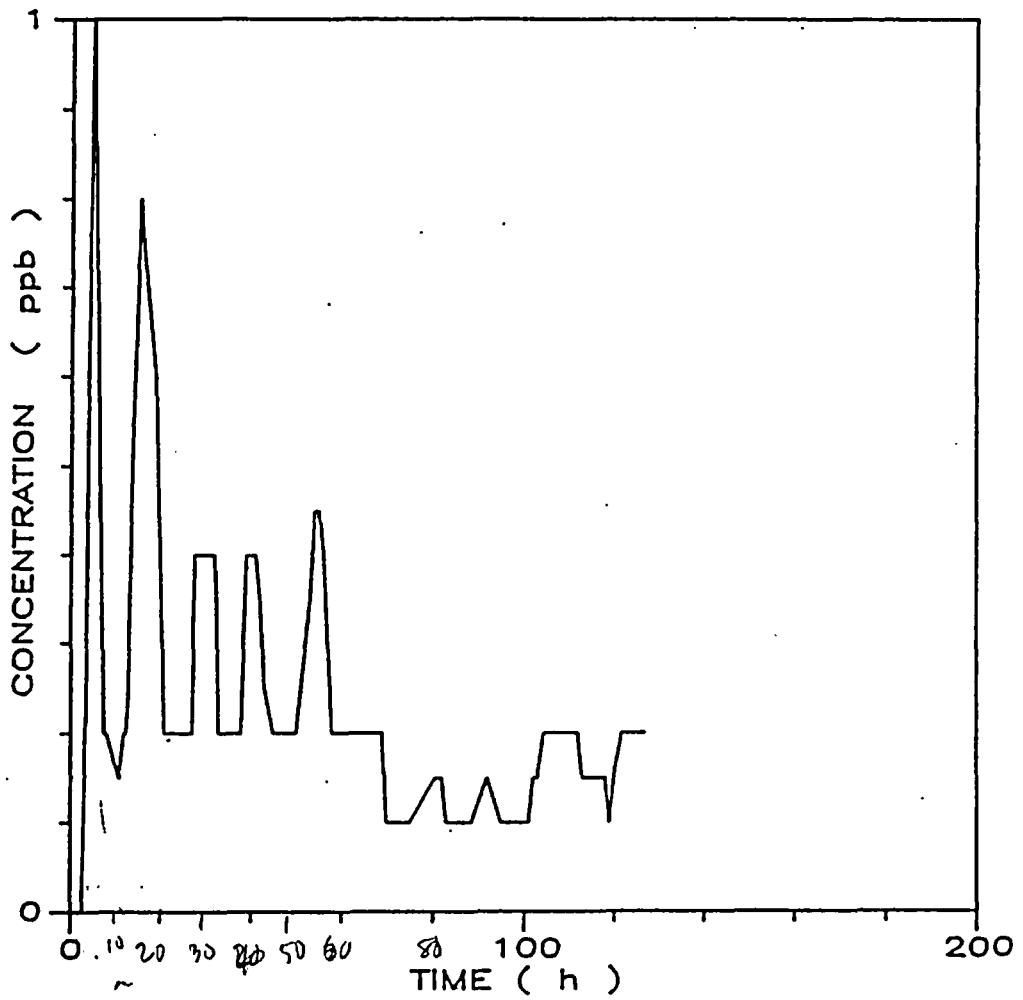

Figure 21 Dye concentration measurements at the Millstone Quarry during Dye Study 2

Table 9

Sensitivity of Entrainment Percentage of Dye to Background Concentration

Background Concentration	% of dye entrained
0.05	34.0
0.08	28.3
0.1	24.4
0.12	20.6
0.15	14.9

2) concentrations at the quarry were measured for 6.5 days after the dye release, our estimate of between 25% and 15% entrainment seems reasonable.

The results of the second dye study can also be compared with our simulation. Recall Table 2, which summarized the simulation of larvae with zero mortality which should correspond approximately with the dye data. Table 2a shows that 21% of the larvae that were hatched were entrained by the plant—in very good agreement with the dye data.

10 Summary and Conclusions

A two-dimesional random walk model was developed to simulate the entrainment, at the Millstone Station, of winter flounder larvae hatched within Niantic River. Important features of the model include larval behavior (vertical migration as a function of time of day and tidal stage) and tidal disperison within the river which was calibrated to Ketchum's (1951) modified tidal prism model. Simulations showed the larvae arriving *significantly earlier*, and *in smaller numbers*, than indicated by observations at the intake. Five hypotheses were suggested as to why this may have happened. These include

1) The input hatching rates are too large

2) The input larval mortality rates are too small

3) Larval residence times within Niantic R. are too short due to either
   a) overestimation of hydrodynamic flushing rates, or
   b) underestimation of larval retention mechanisms (behavior, etc.)

4) The model is underestimating the percentage of larvae within the bay that are being entrained

5) Larvae are being imported from outside the Niantic River area.

Two dye studies were performed to test the hypotheses involving hydrodynamics (3a, 4). The first study, involving a continuous dye release in Niantic River, suggested that the hydrodynamic flushing time is actually *less* than what was simulated so this does not provide an answer. Analysis of all available salinity data supports the dye study. However, a comparison of times of peak abundance of larvae sampled at different stations along the river suggests that the actual larval retention times may be *significantly greater* than the hydrodynamic flushing time, suggesting a greater difference between the transport of larvae and water than we have modeled.

The second dye study, involving a slug release during ebb tide at the river mouth, suggests that the transport of water between the river and the station intake is very rapid (hours to days) and that about 20% ± 5% of all passive particles that exit the river mouth will pass through the intake. This percentage is remarkably close to the value of 21% simulated by the model suggesting that, overall, the model is satisfactorily representing transport within the bay.

Meanwhile, model sensitivity studies show that decreasing the larval mortality factor could partially (but not completely) explain the reduced numbers and early arrival times shown in the simulation. Increasing the larval hatching rates could explain the reduced numbers and, if coupled with increased larval retention (through some mechanism that is presently under simulated), the early arrival times could also be explained. Both discrepancies could also be explained by postulating that larvae are being imported from different spawning areas.

In view of the above conclusions, we feel that further work could be useful in several areas.

Improved Spatial Resolution of Larval Sampling. Several hypotheses for explaining the discrepancy between model simulation and data rest on the assumption that larvae are concentrated near the bottom, where they are presently being undersampled. If this were true in the case of yolk-sac larvae, it could help explain why hatching rates were underestimated. In the case of all larval stages, it would help explain why observed larval residence times are longer than simulated. And the new data could be used to recalibrate the behavioral patterns to eliminate the discrepancy. Additional sampling in the horizontal could also help resolve the spatial distribution of hatching, and provide better input to the bay-wide mass balance as a test of whether or not larvae are being imported.

Calibration of Simulated Residence Times. Our results show that, if calibrated by dye data, the model can faithfully reproduce *hydrodynamic* residence times. However, comparatively little effort has gone into assessing *larval* residence times. Initial evidence is that larval residence times may exceed hydrodynamic residence times by a factor of 5-10, suggesting a strong role for larval behavior. While it may be difficult to directly measure larval residence times in the river, comparisons can be made between simulated and measured larval distribution in space and time. Agreement would confirm the modeled behavior and, once calibrated, the model could be used to simulate larval residence times.

Mortality Rates. Although we have shown that adjustments to mortality are not sufficient to completely explain the model-data discrepancies, our results do indicate strong sensitivity. If questions of larval hatching rates and retention times can be resolved, it will be important to correctly model mortality so that the impact of the station (obtained by comparing simulation with and without power plant entrainment) can be properly assessed. Presently mortality depends only on larval age, but it

properly depends on larval density as well. Incorporation of density-dependent mortality will require some changes in model structure.

References

Adams, E, D. Cosler. 1987. Predicting circulation and dispersion near coastal power plants: Applications using models TEA and ELA. Energy laboratory Report No. MIT-EL 87-008.

Arons, A. B., H. Stommel. 1951. A mixing length theory of tidal flushing. *Transactions of the American Geophysical Union* 32:419-421.

Baptista, A., E. Adams, K. Stolzenbach. 1984. The solution of the 2-D unsteady convective diffusion equation by the combined use of the FE method and the method of characteristics. Report No. 296, Ralph M. Parsons Laboratory, MIT.

Dimou, K. 1989. Simulation of estuary mixing using a 2-D random walk model. S.M. Thesis, MIT Dept. of Civil Engineering.

Ketchum, B. H. 1951. The exchange of fresh and salt waters in tidal estuaries. *J. Mar. Res.* 10:18-37.

Kollmeyer, R. C. 1972. A study of the Niantic River estuary, Niantic, Connecticut. U.S. Coast Guard Academy, New London, Connecticut. Report No. RDCGA 18.

NUEL. 1988, 1989. Monitoring the marine environment of Long Island Sound at Millstone Nuclear Power Station. NUEL, Waterford, Conn.

NUEL. 1988-89. Personal communications.

Officer, C. B. 1976. *Physical oceanography of estuaries.* John Wiley and Sons.

Saila, S. B. 1976. Effects of power plant entrainment on winter flounder populations near Millstone Point. URI-NUSCO Rep. No. 5.

Westerink, J. J., et al. 1984. TEA: A linear frequency domain finite element model for tidal embayment analysis. Energy Laboratory Report No. MIT-EL 84-012.